HEAT AND MASS TRANSFER WITHIN THE DIFFUSION DRIVEN DESALINATION PROCESS WITH HEATED AIR

By

JESSICA KNIGHT

A THESIS PRESENTED TO THE GRADUATE SCHOOL
OF THE UNIVERSITY OF FLORIDA IN PARTIAL FULFILLMENT
OF THE REQUIREMENTS FOR THE DEGREE OF
MASTER OF SCIENCE

UNIVERSITY OF FLORIDA

2006

To my parents, for their infinite support and love throughout my college career.

ACKNOWLEDGMENTS

I would like to thank everyone who has contributed to the successful completion of this work. First, I would like to thank Dr. James Klausner for his constant guidance throughout the past two years and for providing me the opportunity to do research on the diffusion driven desalination project. His patience, academic supervision, and technical assistance are greatly appreciated. I would also like to extend thanks to Dr. Renwei Mei. His academic lectures and technical discussions were always a welcome challenge. I would also like to thank Dr. David Hahn for serving on my supervisory committee.

I would also like to thank all of my peers who helped me through my graduate studies career. A special thanks goes to Yi Li for his assistance and advice.

This research was supported by the U.S. Department of Energy under Award No. DE-FG26-02NT41537. Without their financial assistance this research would not be possible.

Lastly, I would like to thank my parents for their unceasing love and support throughout my academic career. Their constant encouragement and understanding gave me the motivation necessary to achieve my goals.

TABLE OF CONTENTS

LIST OF TABLES

LIST OF FIGURES

NOMENCLATURE

A	Cross sectional area (m^2)
a	Overall specific volume of the packed bed (m^2/m^3)
a_w	Wetted specific area of the packed bed (m^2/m^3)
C_P	Specific heat (kJ/kg-K)
D	Molecular diffusion coefficient (m^2/s)
f	Plant availability
d	Diameter of the tower (m)
d_p	Diameter of the packed bed (m)
G	Air mass flux (kg/m^2-s)
g	Gravitational acceleration (m/s^2)
h_{fg}	Latent heat of vaporization (kJ/kg)
h `	Enthalpy (kJ/kg)
i	Interest rate
K	Thermal conductivity (W/m-K)
k	Mass transfer coefficient (m/s)
L	Water mass flux (kg/m^2-s)
M_v	Molecular weight of vapor (kg/kmol)
m	Mass flow rate (kg/s)
n	Plant life
P	Pressure (kPa)
Pw	Electrical power consumption for pumps (kW)
Q	Retail cost ($)

q_{HL}''	Heat loss flux (kW/m^2)
R	Universal gas constant (kJ/kg-K)
T	Temperature (°C or K)
U	Heat transfer coefficient (W/m^2-K)
V_G	Volumetric flow rate (m^3/s)
γ	Specific cost of operating labor ($\$/m^3$)
μ	Dynamic viscosity (Pa-s)
ρ	Density (kg/m^3)
σ_c	Critical surface tension of the packed bed (N/m)
σ_L	Liquid surface tension (N/m)
ω	Absolute humidity
Φ	Relative humidity
Π	Profit ($)

Subscripts

a	Air
elec	Electricity
evap	Portion of liquid evaporated
fixed	Fixed cost
fw	Fresh water
G	Air/vapor mixture
GA	Gas side parameter based on the specific area of the packed bed
i	Liquid/vapor interface
in	Inlet parameter

L	Liquid
LA	Liquid side parameter based on the specific area of the packed bed
Labor	Labor Cost
LW	Liquid side parameter based on the specific wet area of the packed bed
mix	Air/vapor mixture
out	Outlet parameter
sat	Saturated state
unit,p	Unit amount in terms of production
z	Fluid flow direction

Abstract of Thesis Presented to the Graduate School
of the University of Florida in Partial Fulfillment of the
Requirements for the Degree of Master of Science

HEAT AND MASS TRANSFER WITHIN THE DIFFUSION DRIVEN DESALINATION PROCESS WITH HEATED AIR

By

Jessica Knight

December 2006

Chair: James F. Klausner
Major Department: Mechanical and Aerospace Engineering

The purpose of this research is to examine the performance of the diffusion driven desalination process (DDD) with heated air inlet conditions. A laboratory scale DDD facility has been constructed and fully instrumented. Experiments were conducted and data were collected for two different cases: heated air/ambient water and heated air/heated water. The experiments were conducted over a range of liquid and air mass fluxes. A theoretical heat and mass transfer model was compared against the experimental data collected. The experimental values agree quite well with the theoretical model, provided the fraction of area wetted is correctly specified. The heated air/heated water case is demonstrated to be a more efficient process than the heated air/ambient water case. A parametric study reveals that for every liquid mass flux there is an air mass flux value where the diffusion tower energy consumption is minimal and an air mass flux where the fresh water production flux is maximized. A study was also performed to compare the DDD process with different inlet operating conditions as well

as different packing. It is shown that the heated air/heated water case is more capable of greater fresh water production with the same energy consumption than the ambient air/heated water process at high liquid mass flux. It is also shown that there can be significant advantage when using the heated air/heated water process with a less dense less specific surface area packed bed. A case study with the DDD process was coupled to an industrial site that produces 850,000 acfm heated waste air at 82°C. For inlet air conditions at 82°C, the fresh water production and system energy consumption were both optimal at a diffusion tower liquid mass flux of 0.15 kg/m^2-s, a system air mass flux of 1.5 kg/m^2-s, and a fresh water to air mass flow ratio of 2 in the direct contact condenser. It was determined that with the available energy and operations at the optimal conditions the plant can produce 201,800 gal/day with a total electrical energy consumption of 0.0012 kW-hr/kg and a fresh water production efficiency of 0.224. The total footprint area required is 526.2 m^2. An economic study revealed that the most financial gain can be achieved when the product distilled water is sold as bottled water. Without considering the cost of bottling, if a gallon of distilled water costs $1.00, then a profit of $0.99 per gallon is expected. Thus the DDD process is economically viable when driven by waste heat carried by air.

CHAPTER 1
INTRODUCTION

Water is an essential part of sustaining life on earth, and its use is widespread for industrial, irrigation, mining, and domestic use. While water is abundant on earth, 97% of the water is saline, while only 3% is freshwater. Of the 3% freshwater, 70% of that is frozen in glaciers, ice, or permafrost; 30% is groundwater, while only a mere 0.25% is available above the ground in the form of lakes and rivers. In 2000 Clarke and King [1] estimated that of the 6 billion people on Earth, 0.5 billion people lived in countries that were chronically short on water. It is projected by the year 2050 that the world population will grow to 8.9 billion people and that 4 billion people may live in countries that are chronically short on water. A growing population is accompanied by an increasing need for agricultural and industrial output. Agriculture currently accounts for nearly 70% of freshwater withdrawals, and the demand for food will only increase with increasing population [1]. Growth in industry is also expected. The industrial use of water is expected to grow steeply over the next 25 years as more countries industrialize [1]. Given the fact that the population on earth continues to increase and industrial growth shows no signs of slowing down, it is inevitable that conventional sources of freshwater are not sustainable. The only water resource that is inexhaustible is the oceans. Thus a solution for sustainability may lie in desalination technologies.

Methods of Desalination

Desalination is the process by which salt is removed from water to produce fresh water. There are several different types of desalination, however the two main types are

membrane and thermal- or phase change desalination. Membrane desalination involves the use of a membrane to remove the salt using either electrical force or mechanical force in the separation process. There are two main types of membrane processes: reverse osmosis (RO) and electrodialysis. Unlike membrane processes, thermal desalination removes the salt by causing the solution to undergo a change in phase. Multistage flash (MSF), multiple-effect distillation (MED), and vapor compression (VC) are the most common thermal desalination processes.

Membrane Processes

The most common membrane process is reverse osmosis (Fig. 1-1). Reverse osmosis utilizes a semi-permeable membrane to separate the unwanted ions from the solution. The force driving the solution through the membrane is provided by a feedwater pump whose pressure depends on the concentration of the solid, desired recovery, and overall performance of the membrane. The RO membranes are arranged in pressure vessels often containing 1-7 spiral-wound membrane elements. These vessels can be placed in series or parallel depending on the desired concentration of the final desalted water product.

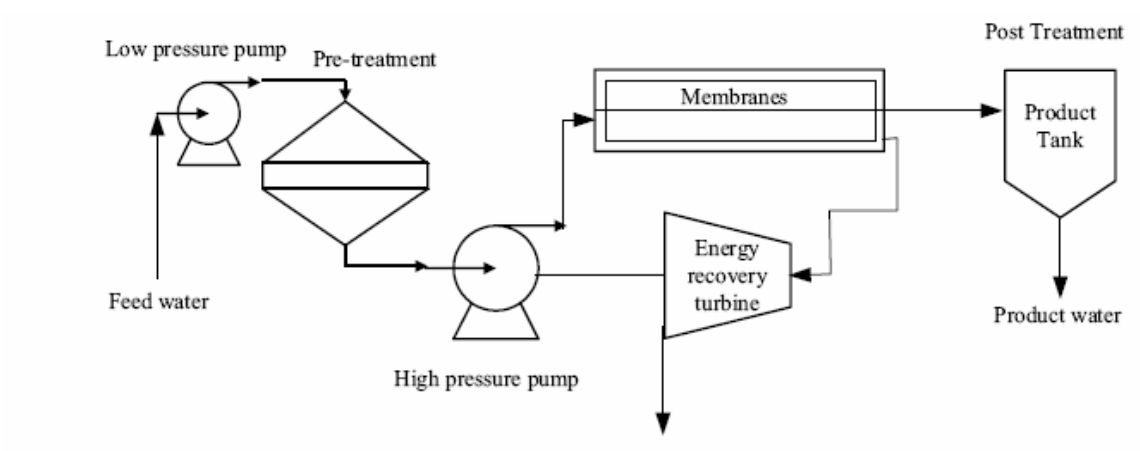

Figure 1-1. Reverse Osmosis (RO) system [2].

Another type of membrane process is electrodialysis, (ED). Unlike RO, ED uses an electrical force to drive the ions through the membrane. It is an electrochemical process where electrodes are placed in a solution of the dissolved solid and a dc power is supplied. The ions will migrate towards the electrode of opposite charge of the given ion. The movement of ions is controlled by ion-selective membranes that form watertight compartments. These membranes are electrically conductive and impermeable to water under pressure.

Thermal Processes

Multistage flash (MSF) is the most widely used thermal process. The MSF process is initiated by heating seawater using steam flowing over the water tubes. The water tubes are enclosed in a vessel called the brine heater. The water then flows to another chamber where the pressure is lowered to the point where the water will either boil or flash into steam. In general there is not a sufficient amount of vapor formed thus several evaporative stages are needed to produce more steam. The steam produced is usually condensed on the heat exchanger tubes running through each stage producing freshwater. Fig 1-2 depicts a schematic diagram of a sample MSF desalination plant.

Multi-effect distillation (MED) and vapor compression (VC) evaporation are other types of thermal distillation processes that are used. MED is quite similar to MSF except in MED, except feedwater is sprayed on the outer surface of the steam tubes to enhance boiling or flashing. VC is generally used for small scale freshwater production and is very similar to MED. However unlike MED, VC typically utilizes mechanical energy, via a mechanical compressor, rather than direct energy to supply the thermal energy to heat the incoming feedwater. The mechanical compressor creates a vacuum in the vessel

and compresses the vapor removed from the vessel. As the vapor exits the vessel it condenses on the inside of a tube bundle and releases heat. The feedwater is then sprayed on the tube bundle where boiling and evaporation occurs.

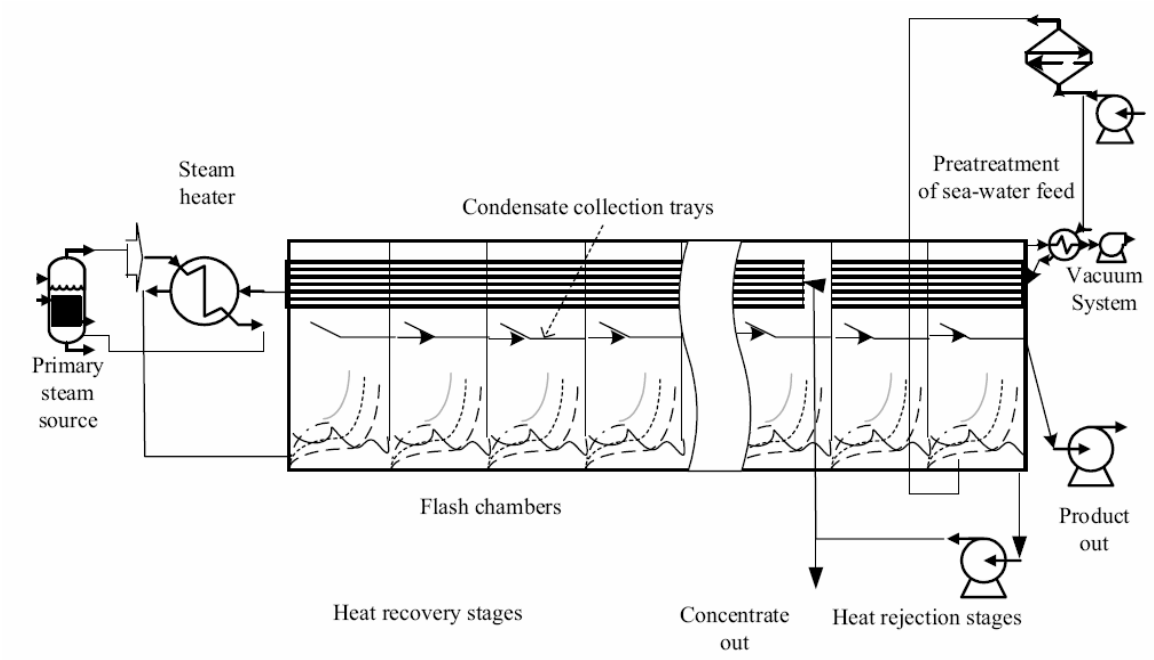

Figure 1-2. Multistage Flash (MSF) plant [2].

Advancements in Desalination

Desalination is a rapidly growing technology. As noted by Mielke and quoted in Dore [3], there are approximately 11,000 desalination plants in 120 countries around the world with a combined capacity of 13.25 Mm^3/d. He also noted the three factors which have the greatest impact on the overall cost of desalination per unit of fresh water produced: salinity of inlet feedwater, energy costs, and plant size. While RO and MSF are still the more widely used methods of desalination there are drawbacks to the processes. The most important is the fact that all of the processes are very energy intensive and are generally only useful for large scale production. With large energy requirements, cost is certainly an issue. John Keys, commissioner of the Bureau of

Reclamation, has said that "cost reduction is the single most important factor to increase the implementation of desalination [4]." Table 1-1 presents a comparison for the costs of the various desalination processes [5]. As the table shows energy demands of the various processes can be extensive. Thus a need emerges for a more energy efficient desalination process.

Table 1-1. Comparison of energy consumption for desalination processes.

Process Type	Distillation			Membrane	
Desalination Process	MSF	MED	MVC	RO	ED
Thermal Consumption, kWh/kg	0.070-0.084	0.042-0.061	-	None	None
Electrical Consumption, kWh/kg	0.0035-0.005	0.0015-0.0025	0.0015-0.002	0.005-0.009	

Of recent interest is a fairly new process entitled humidification dehumidification (HDH). Bourouni et al. [6] describes the process as simple and flexible with low installation and operating costs and encompasses a possibility of utilizing a low temperature energy source. In this process air is drawn through a packed bed tower, the humidifier, where air and preheated seawater will meet and heat and mass transfer will occur creating a saturated air/vapor mixture. The air/vapor mixture then moves to the de-humidifier where the vapor is condensed out. The extraction of the vapor from the air can be done in several ways including mechanical, refrigeration, adsorption, and absorption methods. The most common method is through film condensation used by Bourouni et al. [7]. He reported on an aero-evapo-condensation process using waste geothermal heat and commented on the economic competitiveness of the process. Table 1-2 summarizes his results. From the table it can be seen that the HDH principle is competitive when coupled with the energy from waste heat.

Bourouni et al. [6] commented on the numerous advantages of HDH over other common forms of desalination. First, HDH is flexible in capacity. In general, the only components required are an evaporator and a condenser which can be designed to be compact. Also, due to the low temperature and pressure operating range, components are primarily plastics which are light, inexpensive, and easy to clean. Perhaps most important however is the fact that it can run off of low grade heat which implies that the only energy required for the system is the pumping power.

Table 1-2. Cost estimation per cubic meter of water for various processes.

Plant	Unit Water Cost/m^3
MSF with back-pressure steam turbine	1.57
MSF with gas turbine and waste-heat boiler	1.44
MSF/TVC with gas turbine and waste heat boiler	1.31
RO single-stage with energy recovery	1.39
Aero-evapo-condensation process (geothermal energy)	1.15
Aero-evapo-condensation process (fuel)	4.80

Employing the principles of HDH, a similar process, multiple effect humidification, was developed. This process utilizes the same principles of HDH with the addition of multiple evaporation and condensation cycles. Al-Hallaj et al. [8] reported on a MEH unit utilizing solar collection panels to provide the heating source for the water. They tested both a pilot and a bench unit over a range of operating conditions. They concluded that an increase in water flow rate will maximize the production of the unit to an optimum point, but will also decrease the operating water temperature which leads to a decrease in efficiency of the evaporator and condenser. They also determined that the amount of freshwater produced was directly related to the season. They were also able to increase the production at night by utilizing the hot water rejected from the humidifier.

Vlachogiannis et al. [9] reported on mechanically intensified evaporation (MIE) utilizing the HDH principle in combination with vapor compression and a heat pump. In the MIE process air enters an evaporation chamber through a porous media and is dispersed in small bubbles through the liquid. The exiting stream is then compressed by a blower and directed to a shell and tube heat exchanger. They reported adequate results, but improvements in the condenser surface area were needed to yield a cost effective process.

While HDH shows promise it has its downfalls in comparison with the more well known methods of desalination. First, the overall production rate is smaller in comparison with RO and MSF and thus cannot compete for large scale production. Second, in general natural draft is relied upon for the air. This results in lower heat and mass transfer coefficients as well as an increase in the area of the humidifier. Finally, a shell and tube type heat exchanger is typically used as the de-humidifier. This method of heat exchange directly depends on the amount of surface area. For large freshwater production, more condenser surface area is required which translates to an increase in the amount of land needed.

Thus a more efficient means of desalination should be used to overcome the limitations of the HDH method. Klausner et al. [10] described a diffusion driven desalination (DDD) process that may provide an economically feasible solution to the shortcomings of HDH.

Li et al. [11] describes the DDD process, which is designed to run off of waste heat and is depicted in Figure 1-3.

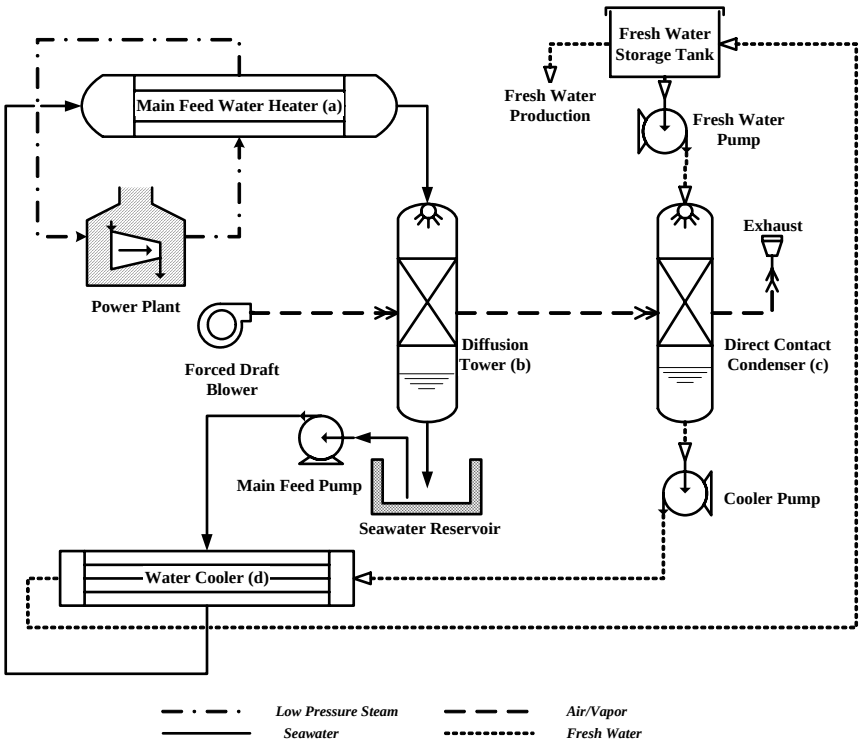

Figure 1-3. Flow chart of the DDD process [11].

The process consists of three main flow lines: the inlet seawater, the air/vapor mixture, and the freshwater. The seawater is drawn from near the surface of a geothermally stratified seawater source and then pre-heated in a water cooler (d). The importance of drawing the water from the stratified source is that the water that is on the surface is much warmer than that at deeper depths due to the solar absorption at shallower depths and thermal stratification. It then flows to the main heater (a) where it is heated using waste heat. Low pressure condensing steam from a thermoelectric power plant is one possible source of waste heat. Once heated, the seawater is then sprayed through the diffusion tower (b) that contains low-pressure drop, high surface area packing material. Simultaneously, a forced draft blower impels the air/vapor mixture through the diffusion tower where a portion of the seawater will evaporate in the air/vapor mixture. The seawater that is not evaporated will exit the diffusion tower as brine discharge. The

saturated air/vapor mixture will enter the direct contact condenser (c) which is the innovative idea behind DDD. As compared to HDH, a direct contact condenser approach is taken to overcome the amount of surface area that would otherwise be required for a shell and tube type heat exchanger. The direct contact condenser allows direct contact between the air/vapor mixture and water thereby improving the heat and mass transfer of the process. A portion of the freshwater product is used to condense the saturated air/vapor as the cooling agent. The freshwater produced will exit the condenser and be pumped to the water cooler where it will be cooled by the feed seawater. A portion of the cooled freshwater is delivered back to the condenser, and the remaining freshwater is then dumped into the freshwater reservoir as product.

The key differences in the DDD process and the HDH process are:

1. A direct contact condenser, in lieu of a shell and tube heat exchanger, is used to decrease the amount of surface area required to condense the air/vapor mixture and increase the condensation effectiveness. The decrease in size of the condenser contributes to less required material as well as less required land space.

2. The DDD process is driven by waste heat from power plants, however, it can be designed to be geography specific depending upon the location. For example, other forms of waste heat may be used such as solar heating, geothermal spas, or wind turbines may be used.

3. Forced draft is used in combination with a packed bed tower as the humidifier. The forced draft provides a constant source of dry air. The packed bed is designed to be made of plastic due to the low operating temperature and pressure. Plastics are easier to maintain as well as cheaper to replace. The packed bed also provides an increase in surface area for more heat and mass transfer between the air and water and thus greater production.

4. The HDH process is compatible for only small scale production whereas the DDD process can be used for larger flow rates and thus at a larger scale for increased production.

5. The components used for the DDD process are commonly available from a variety of different manufacturers or retailers.

Given the advantages of DDD over the HDH process it is worthwhile to research the overall production rates and economic feasibility of the process.

Desalination and the Environment

Water desalination has increased substantially throughout the 20th century. With this increase has come an improvement in the quality of life. This improvement, however, comes at a price. The price is paid through the damage done to the environment. Water desalination contributes in a multiple of different ways to the degradation of the environment. These include increased occupation of land by desalination plants, the contamination of groundwater, damage done to marine biology, noise pollution, and the energy and discharge of combustion of products all have a negative impact on the environment.

In a world where the population is steadily increasing and total land remains constant, land use and occupation is always an issue. For example, Sadhwani et al. [12] noted that a typical RO plant requires a land area of about 10,000 m^2 (2.47 acres) to produce between 5,000-10,000 m^3/day (1.32 million gal/day to 2.6 million gal/day). In addition to the land footprint occupied by the plant, the infrastructure of the plant is a concern. The feed seawater pipes, the electrical transmission lines, and the product water pipes are all important parts of the infrastructure that require space and land use.

The groundwater could also face contamination from a desalination plant. A plant that is built over or near an aquifer will have pipes to transport the inlet seawater as well as those for product discharge. These pipes could leak, allowing saltwater to seep through to an aquifer. Care must be taken to ensure no leaks are present. [12].

Morton et al. [13] commented that the marine life can suffer in several ways from the discharge of desalination plants. The brine discharge from desalination plants is

typically of increased temperature and of higher salinity and depending upon treatments used during the process, rich in other chemicals as well. The warmer water and increased salinity can also reduce the amount of dissolved oxygen in the water and therefore restricts marine life in the vicinity of the plant. The presence of other chemicals could intensify this effect. The temperature increase could result in death of marine life or a reduction in the rate of metabolic processes which retards maturity, life stage development, and size. Morton et al. [13] concluded that thermal desalination processes are more prone to have a greater thermal impact on the environment whereas membrane processes typically have a greater salt concentration of the discharge.

The noise from a desalination plant is a concern in the vicinity surrounding the plant as well as to the workers of the plant. This acoustic contamination is primarily an issue for RO plants where high pressure pumps and energy recovery systems can produce noise in excess of 90 dB(A) [12].

Of perhaps greatest importance is the atmospheric emissions from the input energy. Recall Table 1-1 and the substantial amount of input energy required for various desalination processes. These processes generally rely on the combustion of fossil fuels to supply the necessary energy. The principle emissions from the combustion of fossil fuels are sulfur dioxide, nitrogen oxides, carbon dioxide, carbon monoxide, and suspended particulate matter [13]. From Table 1-1 it can be seen that the MSF is more energy intensive when compared with RO and thus more likely to contribute to air contamination.

Comparison of DDD with RO and MSF

It is obvious that economics as well as environmental concerns play an important role in the viability of desalination processes. One of the biggest advantages of DDD

over RO and MSF is that DDD is driven by waste heat, therefore the only energy required is that to pump the air and water through the system. Since low pressure drop packing is used the energy required for pumping is not prohibitively expensive. This has very important implications for the environment. DDD takes advantage of energy that would have otherwise been discarded. Since it does not require as much energy as RO or MSF it is expected that the atmospheric emissions will be significantly less. Breschi [14] reported on the performance of a desalination unit called LTF (low-temperature flash) that ran off of waste heat. The unit consists of a vacuum flash chamber (the evaporator), a shell-and-tube exchanger (the distillate condenser), and a vacuum system. The process is driven by the small temperature difference in the warm seawater exiting a steam turbine. The environmental impact of that facility was considered negligible due to the low change in salinity of the brine and the lack of chemical additive to reduce scaling since the operating temperature is low.

Another advantage of DDD is that the main components are inexpensively manufactured. The operating temperatures and pressures are low; therefore most parts can be constructed from simple plastics. Unlike RO, there are no membranes that must be changed and maintained. While RO and MSF require specialized high pressure and large pumps respectively.

The DDD process has the potential to be economically competitive while having less impact on the environment. The scope of this research is to explore the feasibility of the DDD process under specific operating conditions.

Scope of Work

Li et al. [11] reported on the economic feasibility of the DDD process with heated input feedwater and ambient dry air. The purpose of this research is to explore the

concept of a heated dry air input. It is known that the amount of vapor carried by the air increases with increasing temperature, but further studies need to be conducted to determine the effect of a heated air input on the DDD process. Thus the goals of this study are as follows:

1. Design and install an air heated section to the DDD facility that is fully instrumented to measure the appropriate heat and mass transfer rates.

2. Take experimental measurements over a range of flow conditions for two separate cases: the case where both inlet air and inlet feedwater are heated and the case with a heated air input with an ambient water input.

3. Develop and implement a mathematical model to correctly predict the heat and mass transfer behavior of the two cases.

4. Perform a parametric study to determine the optimal operating conditions.

5. Perform an economic study to determine the practicability of the DDD process for the two different cases.

Chapter 2 describes the DDD process constructed and maintained for the current research. The instrumentation, the individual components, and software used to collect the data are all described in detail.

A theoretical model for a heated air input for both an ambient water input as well as a heated water input is presented in detail in Chapter 3. A control volume approach is taken to reduce the conservation equations to determine the governing equations of the two processes. The results for the two different cases will then be compared to the model and then discussed.

Finally, in Chapter 4, the results from a study to determine the optimal conditions for both cases are presented. The economics of the process are also explored in an example of the DDD process coupled with an industrial plant.

CHAPTER 2
EXPERIMENTAL FACILITY

A laboratory scale diffusion driven desalination (DDD) facility has been designed and constructed to collect the heat and mass transfer data for the experimental analysis. The data collected will be used to verify the theoretical model for the diffusion tower for two different cases: heated air/heated water and heated air/ambient water. Data for both cases will be taken over a range of different flow conditions. The performance of both cases will then be explored using the data collected.

System Overview

Figure 2-1 presents a schematic diagram of the current DDD facility. The municipal water line, serving as the inlet source water, flows through a series of valves which determines the flow meter to measure the inlet mass flow rate. The water then flows through a series of heaters, the preheater and the main heater. The preheater can raise the temperature to a maximum of 50 °C and the main feedwater heater is a PID temperature controlled heater. Once the water is heated, its temperature is measured and then it flows into the top of the diffusion tower. The water is sprayed with a spray nozzle and flows through the tower packing via gravity. The water not evaporated will exit the tower from a drain at the bottom where the temperature is measured using a type E ungrounded thermocouple.

The dry air is drawn through a 3.68 kW (5.0 horsepower) centrifugal blower whose speed is regulated using a three phase autotransformer. The air exiting the blower flows through a 10.2 cm nominal vertical duct where a thermal mass flow rate meter measures

the air flow rate. The major modification to the system described by Li [15] is the addition of an air heating section. The air heating section is shown pictorially in Fig. 2-2. The U-shaped air heater section is required to ensure enough pipe length for fully developed flow for the air flow measurement. The air flow meter is placed before the air heater since it was calibrated using ambient air. The air flows down the duct where a 4 kW tubular heater is installed. A thin sheet of aluminum lines the inside of the duct to guarantee that the duct does not exceed its maximum operating temperature. The amount of power supplied to the air heater is controlled by a single-phase autotransformer. The

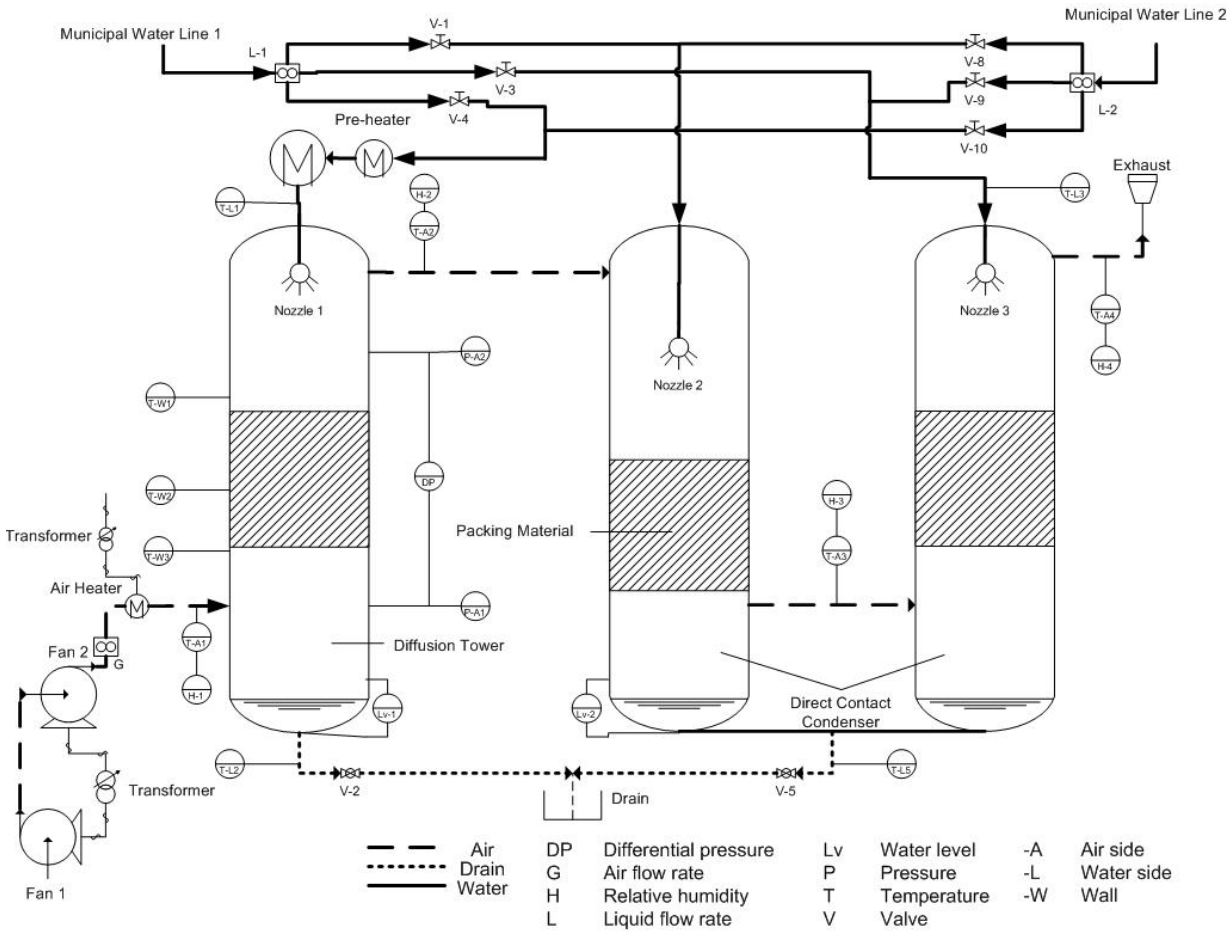

Figure 2-1. Diffusion driven desalination (DDD) facility.

air relative humidity and temperature are then measured using a resistance type humidity gauge located downstream of the flow meter and heater in the horizontal section. The air then enters the diffusion tower and is forced through the packed bed. The air exits the diffusion tower where the exit relative humidity and temperature are measured in a similar manner as at the entrance.

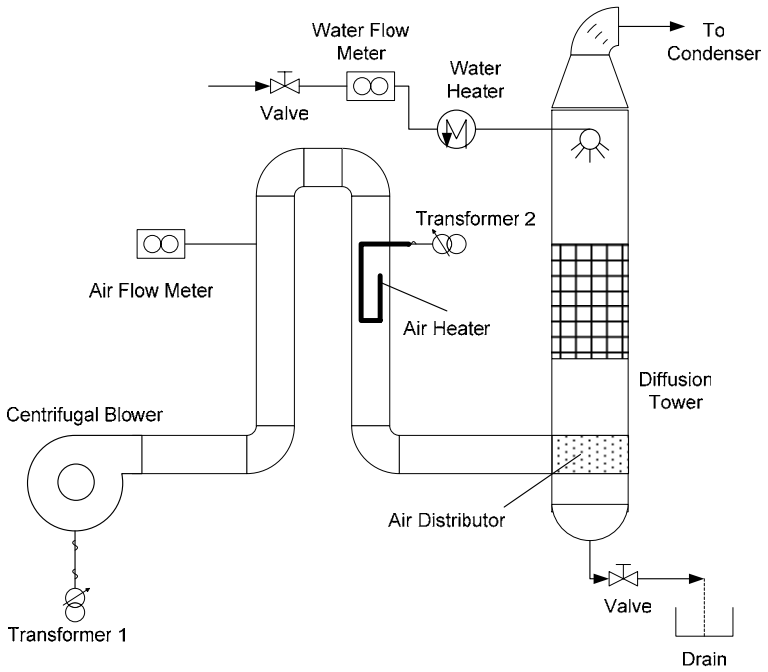

Figure 2-2. Air heating section.

The condenser is comprised of two different stages: a countercurrent stage and a co-current stage. The condenser is designed in a twin tower structure where both towers are identically constructed. Both towers are made of 25.72 cm inner diameter acrylic tubing connected via two schedule 80 PVC elbows. Though this study only focuses on the performance of the diffusion tower, the condenser is included for completeness of the system.

Fresh cold water is drawn from a different municipal line and split into two different lines, one line for each section of the condenser. The water flow rate is measured with two different turbine flow meters. The water temperature is measured and then the water is sprayed from the top of both of the towers using additional spray nozzles.

The air leaving the diffusion tower is at an elevated temperature and humidity. The air enters the co-current condenser stage where the air flows co-currently with water and is cooled and de-humidified. Upon exiting the co-current stage, the air will flow through a 90° PVC elbow where it travels through a 25.4 cm nominal diameter duct. The air temperature and humidity is measured with another resistance type humidity gauge as was used in the diffusion tower. The air then enters the countercurrent stage where the air flows upward in the opposing direction of the falling water and continues to further cool and dehumidify. The exit air temperature and humidity are measured with another gauge and the air will then exit via a duct at the top of the countercurrent condenser stage.

The water used to cool the air in the condenser and the condensate product from the air will flow down in both towers to a drain where the exit water temperature is measured. Fig. 2-3 depicts a pictorial view of the DDD facility.

Description of Individual Components

The diffusion tower, shown in Fig. 2-4, is composed of three primary sections: the top, middle, and bottom. The bottom consists of the air entrance and drain, the middle houses the packing, and the top contains the water spray and exit air duct. The middle portion of the tower is composed of 27 cm outer diameter 0.64 cm thickness R-Cast cast acrylic tube. The packed bed of the tower can occupy up to 1 m of height in the acrylic tube. The bottom and the top portions are schedule 40 25.4 cm nominal PVC pipe.

The bottom and middle portions of the tower are connected via a schedule 80 PVC 25.4 cm nominal bolted flange.

Figure 2-3. Diffusion driven desalination (DDD) system.

The condenser stage of the DDD system is comprised of two different stages each with a top segment connected to a common bottom segment. The top segments include the actual tower, the water spray, and the air duct, while the bottom segment contains the drain and packed bed sections. The towers of both stages are also composed of 27 cm outer diameter 0.64 cm thickness R-Cast cast acrylic tube. The two segments are connected via schedule 80 PVC 25.4 cm nominal sized bolted flanges. The bottom portion contains two schedule 80 90° 25.4 cm PVC elbows connected using a 25.4 cm nominal size schedule 40 PVC pipe. Up to 50 cm of packing material can be accommodated in each vertical portion of the bottom segment.

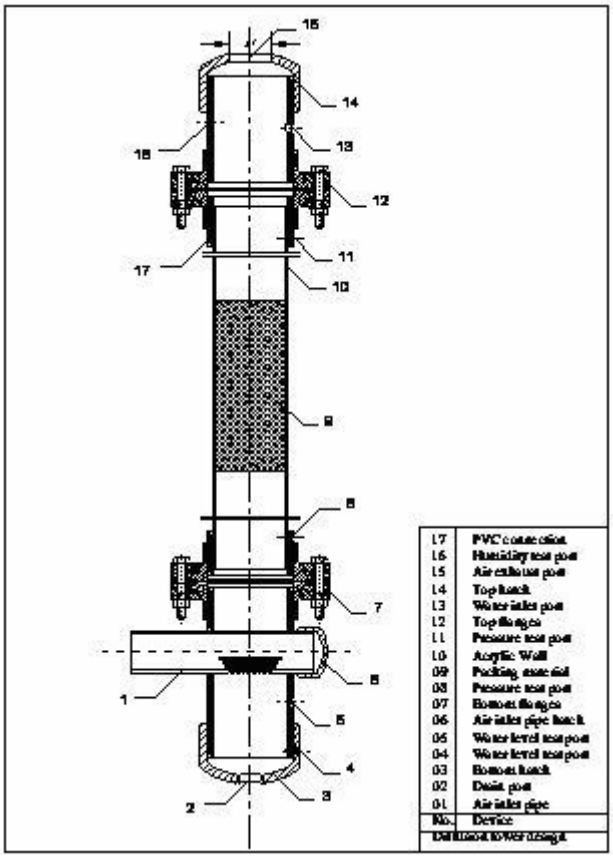

Figure 2-4. Diffusion tower [15].

The three water distributors used in the diffusion tower and direct contact condenser are manufactured by Allspray. They are brass full cone with a 65° spray angle and are designed for uniform solid cone spray. The two spray nozzles used for the direct contact condenser have a capacity of 7.57 lpm (2.00 gpm). Fig. 2-5 illustrates a typical Allspray nozzle.

The water preheater is a DHC-E tankless electric water heater manufactured by Stiebel Eltron. It is a 240 V heater where the input of heat is electronically controlled. Its operating range is from 30° C to 52° C.

Figure 2-5. An Allspray water distributor.

The main water heater consists of two 3 kW electric coil heaters wrapped around a copper pipe where the water flows. The heater is PID controlled with a 240 V output. The feedback is controlled with a type J thermocouple located at the exit of the heater.

The air heater is a 4 kW 1.21 cm diameter round cross section tubular heater. It has a 240 V rating and has a watt density of 194 W/cm^2. The sheath is Incoloy, which has a maximum temperature of 815°C. It has a sheath length of 254 cm and a heated length of 236 cm. The heater has been shaped to fit inside the 9.5 cm inner diameter pipe. Figure 2-6 shows the heater shape. The power to the heater is controlled with a single-phase autotransformer.

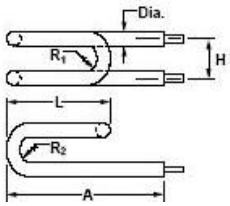

Figure 2-6. Shaped heater.

The packed bed is high density, low pressure drop HD Q-PAC type from Lantec. It is made of polypropylene and is available in 30 cm x 30 cm x 30 cm square pieces. The packing material was cut to fit the round acrylic tubes of the diffusion tower and direct

contact condenser towers using a specially designed hot wire setup. It has a specific diameter of 18 mm and a specific area of 267 m^2/m^3. Figure 2-7 shows a portion of the packed bed cut for use in the system.

Figure 2-7. The HD Q-PAC packed bed.

The three turbine water flow meters used to measure the water flow rate in the DDD system are manufactured by Proteus Industries Inc. Two flow meters have a flow range of 5.7-45.4 lpm (1.5-12.0 gpm) while one flow meter has a range of 0.4-3.8 lpm (0.1-1.0 gpm). They require a 24 VDC input and have a 0-5 V or 0-20 mA output. All have an accuracy of ±1.5% full scale and were calibrated using the catch and weigh method. Figure 2-8 shows the calibration curves obtained for the three different flow meters.

The air flow meter is a thermal insertion mass flow meter (Sierra Series 620S Fast-Flo) from Sierra Instruments Inc. It has a microprocessor-based transmitter for 0-10

VDC output and a 200 s response time. It has a 15.24 cm 304 stainless steel probe to measure velocity as well as temperature. The flow meter range is 0-1125 SCFM of air with an accuracy of ±1% full scale. The flow meter was delivered as factory calibrated.

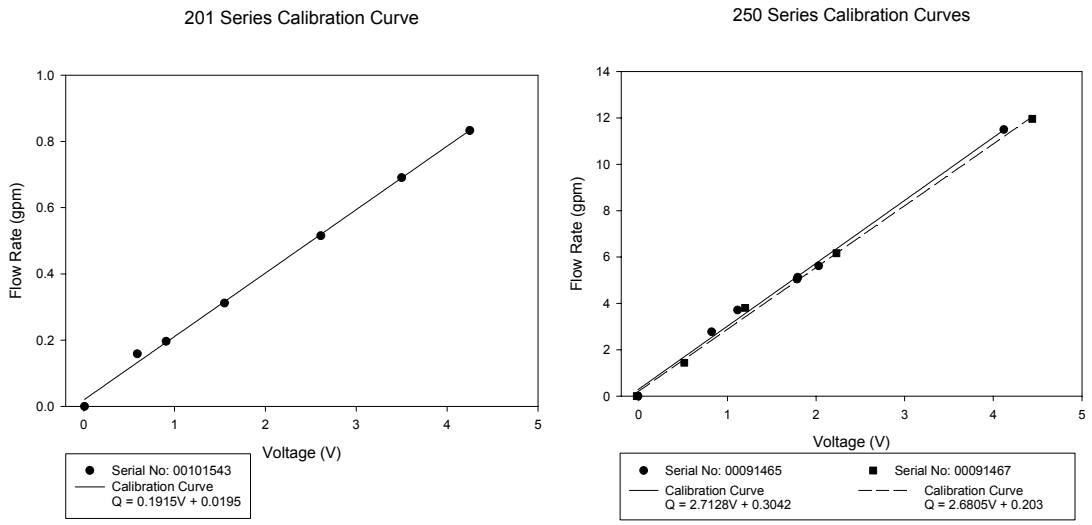

Figure 2-8. Water flow meter calibration curves.

There are four Vaisala Corp. HMD70Y resistance type humidity gauges to measure the relative humidity as well as temperature. Both temperature and humidity have transmitters for 0-10 V output. All four gauges were factory calibrated. The operating range for temperature is -20° to +80° C, while the relative humidity has an operating range of 0-100%. The uncertainty of the gauges is ±1° C for temperature and ±2% relative humidity.

The thermocouples used in the facility are type E and were manufactured by Omega. They are factory calibrated with an uncertainty of ±0.2° C.

The data acquisition system consists of a 16-bit PCI Analog-Digital converter and a 32 channel multiplexer card manufactured by Measurement Computing. The board is calibrated for type E thermocouples and has a 0-10 V input range.

The data acquisition system uses the program SoftWIRE to collect the necessary heat and mass transfer data. The SoftWIRE editor uses constructed flow diagrams to represent the flow of data and control with icons and wires. The program developed for the DDD system includes five different interfaces: the main control, the diffusion tower view, the direct contact condenser view, the diffusion tower histogram view and the direct contact condenser histogram view. The SoftWIRE program sends all of the data directly to an Excel spreadsheet where the data is collected.

The main control tab of the DDD program allows direct control over the program. A view of the main control is depicted in Figure 2-9. There is an on/off switch to turn the program on as well as a frequency box to input the desired data sampling rate. It also depicts specific values important to the overall process. Values specific to the diffusion tower are depicted in the diffusion tower tab while those specific to the direct contact condenser are shown in the diffusion tower tab. Figure 2-10 shows the diffusion tower tab. As the picture illustrates, values at certain locations of the diffusion tower are visible and are easily available.

Since steady state is an important assumption in the DDD analysis, it is important to obtain measurements at steady state conditions. Two of the interfaces in the DDD programs include a series of histograms which indicate the degree to which steady-state is achieved. Figure 2-11 shows a view of the diffusion tower histogram view. The x-axis is the time coordinate while the y-axis is the given measured value. All measurements recorded were taken at steady state conditions at a frequency of 1 Hz.

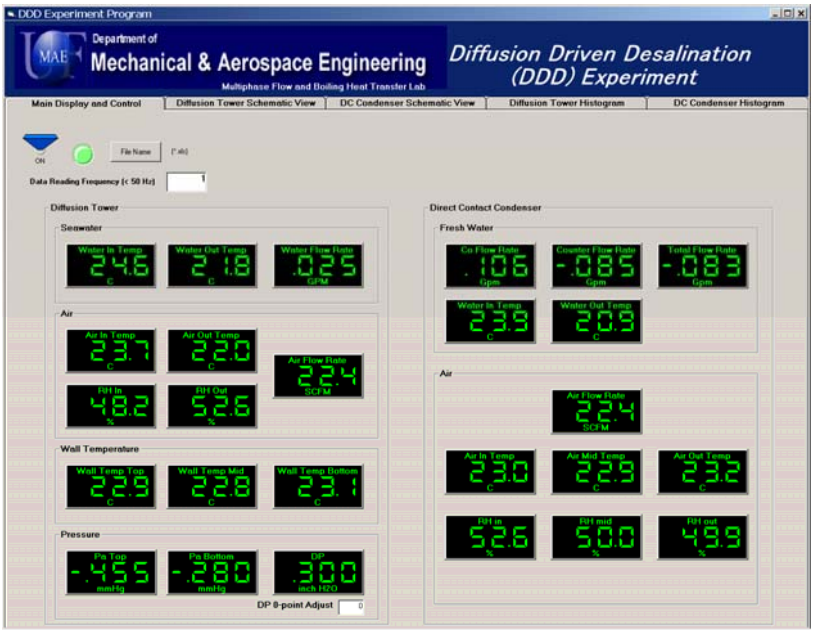

Figure 2-9. Main control.

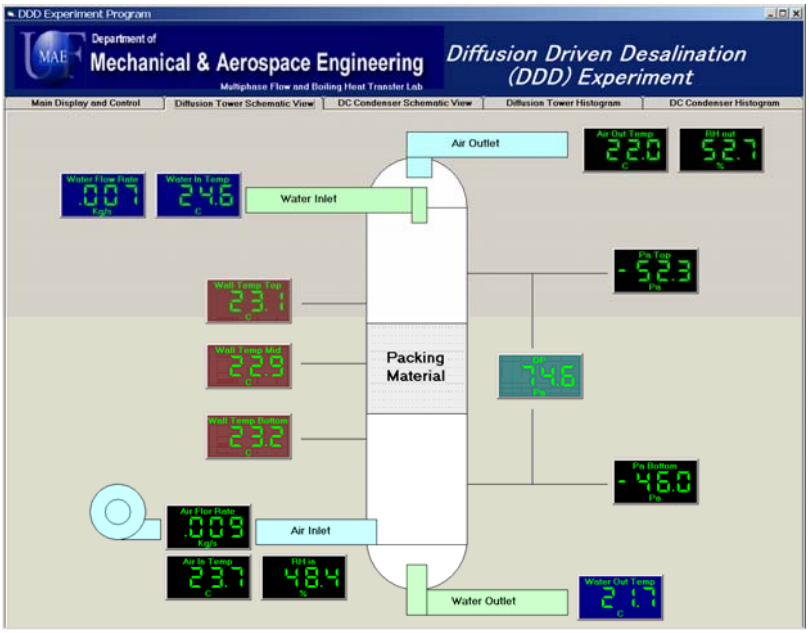

Figure 2-10. Diffusion tower data.

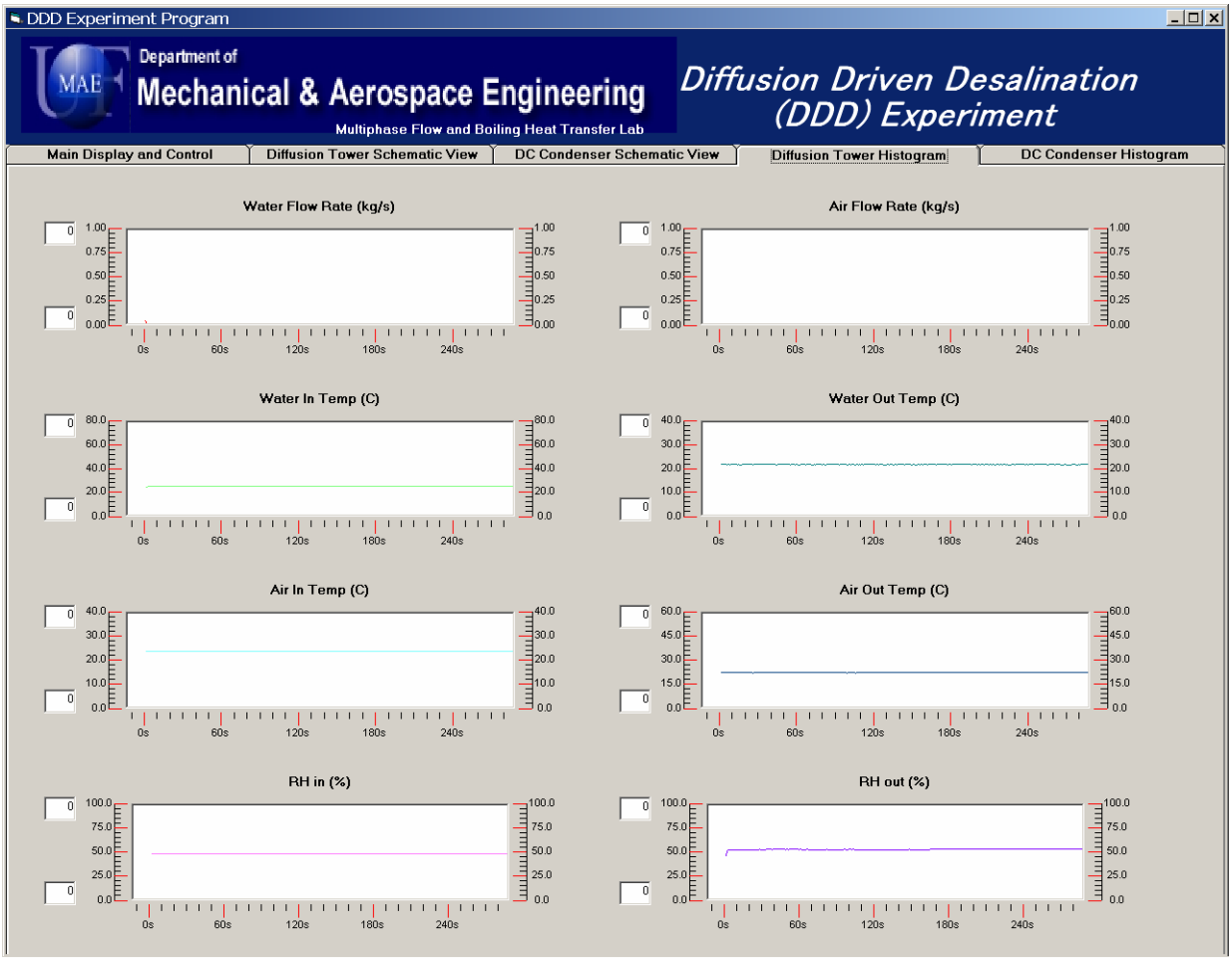

Figure 2-11. Histogram view of the DDD data acquisition.

CHAPTER 3
HEAT AND MASS TRANSFER WITHIN THE DIFFUSION TOWER

An in depth theoretical model for both the diffusion tower [16] and direct contact condenser [17] based on heated water/ambient air inputs has already been explored. The purpose of this analysis is to experimentally explore the performance of the diffusion tower for two different cases: heated air/heated water input and a heated air/ambient water input. The heat and mass transfer model, proposed by Klausner et al. [16] has been investigated for both cases. The theoretical model is compared with the experimental data collected and agreement is satisfactory.

Theoretical Heat and Mass Transfer Model

The theoretical model is a one-dimensional two fluid film model for a packed bed. The conservation equations for mass and energy are applied to a differential control volume to obtain the governing equations for the process. In order to determine the governing equations certain assumptions must be made. The assumptions made are:

1. The process operates at steady-state.
2. Air and water vapor are both perfect gases.
3. The changes in kinetic and potential energy are negligible.
4. The pumping power required for water is solely that required to overcome gravity.

Fig. 3-1 shows the differential control volume analyzed for the two cases. As it can be seen the problem is one-dimensional with the only variation lying in the z-direction.

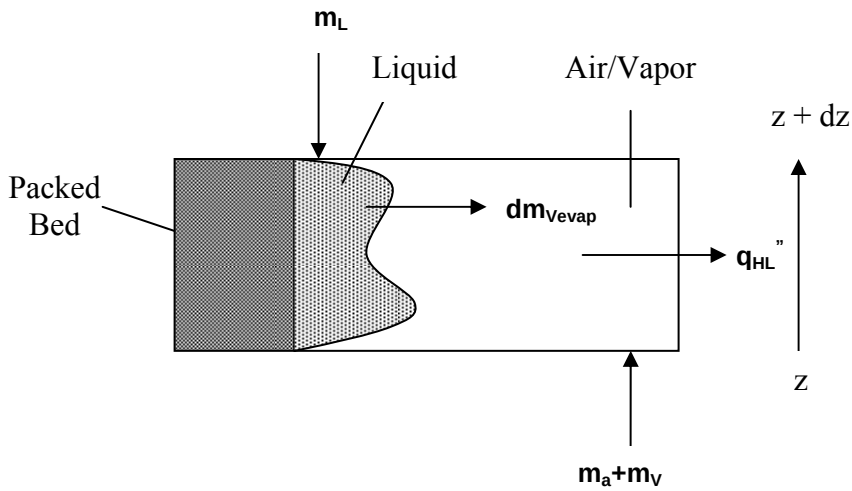

Figure 3-1. Differential control volume for heated air conditions.

The z-direction is taken as positive in the axial direction. The conservation of mass on the control volume for the air/vapor mixture yields,

$$\frac{d}{dz}(m_{V,z}) = \frac{d}{dz}(m_{V,evap}), \tag{3.1}$$

where m represents the mass flow rate, the subscripts V and evap denote vapor and the vapor evaporated from the liquid respectively. Similarly, conservation of mass on the liquid side yields,

$$-\frac{d}{dz}(m_{L,z}) = \frac{d}{dz}(m_{V,evap}), \tag{3.2}$$

where the subscript L denotes liquid.

The humidity ratio, ω, and relative humidity, Φ, are defined for an air/vapor mixture as follows,

$$\omega = \frac{m_V}{m_a} = \frac{0.622\Phi P_{sat}(T_a)}{P - \Phi P_{sat}(T_a)}, \tag{3.3}$$

where P is the total pressure of the system, and $P_{sat}(T_a)$ is the saturation pressure of the vapor evaluated at the air temperature T_a. The small change in system pressure is not accounted for in evaluating the properties. The definition of the mass transfer coefficient is applied to the differential control volume to obtain the following,

$$\frac{d}{dz}(m_{V,evap}) = k_G a_w (\rho_{V,sat}(T_L) - \rho_{V,\infty}(T_a))A, \tag{3.4}$$

where k_G is the gas mass transfer coefficient, a_w is the wetted specific area, and A is the cross sectional area of the diffusion tower. It should be noted that the total specific area of the packing, a, is the total surface area of packing per unit volume of space occupied. The rate of change of evaporation can be further reduced by considering the perfect gas law. By applying the perfect gas law [18] to Equation 3.4, the rate of evaporation becomes,

$$\frac{d}{dz}(m_{V,evap}) = k_G a_w \frac{M_V}{R}\left[\frac{P_{sat}(T_i)}{T_i} - \frac{\Phi P_{sat}(T_a)}{T_a}\right]A, \tag{3.5}$$

where M_V is the molecular weight of vapor, R is the universal gas constant, and T_i is the liquid/vapor interfacial temperature. By combining Equations 3.2-3.5 the gradient of the humidity ratio is,

$$\frac{d\omega}{dz} = \frac{k_G a_W}{G}\frac{M_V}{R}\left[\frac{P_{sat}(T_i)}{T_i} - \frac{\omega}{0.622+\omega}\frac{P}{T_a}\right], \tag{3.6}$$

where $G = \frac{m_a}{A}$ is the air mass flux. Equation 3.6 is a first order ordinary differential equation with dependent variable ω. When solved, the humidity ratio along the axial z direction is obtained. Equation 3.6 requires a value of the liquid/vapor interfacial

temperature, T_i. The interfacial temperature is found by recognizing that the energy convected from the liquid is the same as that convected to the gas,

$$U_L(T_L - T_i) = U_G(T_i - T_a)\,, \tag{3.7}$$

where U_L and U_G are the heat transfer coefficients of liquid and gas respectively. The interfacial temperature is obtained by solving Equation 3.7 and is,

$$T_i = \frac{T_L + (U_G / U_L)T_a}{1 + (U_G / U_L)}\,. \tag{3.8}$$

The conservation of energy on the liquid side of the differential volume yields the following,

$$\frac{d}{dz}(m_L\, h_L) = \frac{d(m_{V,evap})}{dz} h_{fg} + Ua(T_L - T_a)A\,, \tag{3.9}$$

where h is the enthalpy, U is the overall heat transfer coefficient, and h_{fg} is the latent heat of evaporation. Equation 3.9 can be further manipulated by utilizing the following:

$dh_L = C_{pL} dT_L$ and $\frac{d}{dz}(m_L\, h_L) = h_L \frac{d\, m_L}{dz} + m_L \frac{dh_L}{dz}$, and $h_{fg}(T_a) = h_V(T_a) - h_L(T_a)$. The gradient of the liquid temperature, T_L, then reduces to the following,

$$\frac{dT_L}{dz} = \frac{G}{L}\frac{d\omega}{dz}\frac{(h_{fg} - h_L)}{C_{PL}} + \frac{Ua(T_L - T_a)}{C_{PL}L}\,, \tag{3.10}$$

where $L = \frac{m_L}{A}$ is the liquid mass flux, C_P is the specific heat, and a is the overall specific area of the packing material. Equation 3.10 is also a first order ordinary differential that when solved will yield the temperature distribution of the water throughout the diffusion tower.

Likewise, conservation of energy of the air/vapor mixture is obtained from the differential control volume and yields,

$$-\frac{d}{dz}\left(m_a\, h_a + m_V\, h_V\right) + \frac{d}{dz}(m_{V,evap})h_{fg} = -Ua(T_L - T_a)A + q''_{HL}\pi d \tag{3.11}$$

As in the liquid energy equation, Equation 3.11 can be simplified by utilizing the fact that the air mass flow rate is held constant throughout the entire process such that:

$$\frac{d}{dz}(\dot{m}_a\, h_a + \dot{m}_V\, h_v) = \dot{m}_a \frac{dh_a}{dz} + \dot{m}_V \frac{dh_V}{dz} + h_V \frac{d\,\dot{m}_V}{dz},\ \frac{dh_a}{dz} = C_{Pa}\frac{dT_a}{dz},\ \text{and}\ \frac{dh_V}{dz} = C_{PV}\frac{dT_a}{dz}.$$

Equation 3.11 then becomes,

$$-\frac{dT_a}{dz}(m_a\, C_{Pa} + m_v\, C_{PV}) = h_L(T_a)\frac{d\,m_v}{dz} - Ua(T_L - T_a)A + q''_{HL}\pi d\ . \tag{3.12}$$

Equation 3.12 can be simplified by noting that the C_{Pmix}, specific heat of the mixture, is evaluated as,

$$C_{Pmix} = \frac{m_a}{m_a + m_V}C_{Pa} + \frac{m_V}{m_a + m_V}C_{PV} \tag{3.13}$$

Recalling the evaluation of the latent heat of evaporization from the liquid conservation equation, and combining Equations 3.12 and Equation 3.13 the gradient of air temperature through the diffusion tower is evaluated as,

$$\frac{dT_a}{dz} = -\frac{1}{1+\omega}\frac{d\omega}{dz}\frac{h_L(T_a)}{C_{Pmix}} + \frac{Ua(T_L - T_a)}{C_{Pmix}G(1+\omega)} - \frac{4q''_{HL}}{Gd(1+\omega)C_{Pmix}} \tag{3.14}$$

where d is the diameter of the diffusion tower and q''_{HL} is the heat flux loss from the air. Equation 3.14 is also a first order ordinary differential equation with dependent variable T_a. Equations 3.6, 3.10, and 3.14 are a set of coupled ordinary differential equations that when solved simultaneously give solutions for the distributions of humidity ratio, air

temperature, and water temperature throughout the diffusion tower. However, since a one-dimensional model is utilized, closure must be achieved. This requires that both the heat transfer coefficient and mass transfer coefficient be known. Directly measuring the heat transfer coefficients is not possible because of the fact that the interfacial film temperature cannot be measured. Therefore to overcome this difficulty the heat and mass transfer analogy [19] has been utilized. The heat transfer coefficient for the liquid side is evaluated using,

$$\frac{Nu_L}{\mathrm{Pr}_L^{1/2}} = \frac{Sh_L}{Sc_L^{1/2}} \tag{3.15}$$

$$U_L = k_L \left(\rho_L C_{PL} \frac{K_L}{D_L} \right)^{1/2} \tag{3.16}$$

Similarly, the heat transfer coefficient for the gas side is calculated as,

$$\frac{Nu_G}{\mathrm{Pr}_G^{1/3}} = \frac{Sh_G}{Sc_G^{1/3}} \tag{3.17}$$

$$U_G = k_G \left(\rho_G C_{PG} \right)^{1/3} \left(\frac{K_G}{D_G} \right)^{2/3} \tag{3.18}$$

where D is the molecular diffusion coefficient and K is the thermal conductivity. Thus the overall heat transfer coefficient is evaluated as,

$$U_L = \left(U_L^{-1} + U_G^{-1} \right) \tag{3.19}$$

The mass transfer coefficient is evaluated using a widely known and well tested correlation. Onda's correlation [20] allows for evaluation of the mass transfer coefficients in packed beds. Onda's correlation, found in Appendix A, is used to calculate the mass transfer coefficients, k_G and k_L. In the correlation the coefficient, C, can take on two possible values C=5.23 for $d_p > 15$ mm and C=2.00 for $d_p \leq 15$ mm.

The difference in C values accounts for the fact that $k_G a$ for the smaller packing ($d_p \leq 15$ mm) tends to increase monotonously with increasing specific area, a. Li et al. [17] provided an explanation for the phenomena of the decreased mass transfer coefficient and is believed to be the cause of liquid hold-up in the packed bed which is responsible for liquid bridging and reduced area for mass transfer. The current packed bed has a diameter of 18 mm which is close to the cut off for both sizes. Thus for the packed bed used in the current investigation, either constant value would be appropriate. Similar to the analysis described by Klausner et al. [16], the heated air/ambient water uses C=5.23. The coefficient for the heated air/heated water case, however, uses C=2.0. This change in constant can perhaps be attributed to the fact that at higher air temperatures the air that enters the packed bed is dryer and thus more water is evaporated. However, due to the increase in evaporation there is an increased hold up of the liquid in the packing due to an accelerating gas stream. The increase in hold up could possibly cause more liquid bridging in the packing thereby decreasing the local mass transfer.

The wetted area for the current experiments differs from that computed via Onda's correlation. It was found that the specific wetted area remains nearly constant for varying air to water mass flow ratios. This was determined by first using Onda's correlation to calculate the wetted specific area. There was slight variation in the comparison of the theoretical and experimental data. An analysis was then performed to determine what the specific wetted area should be to obtain adequate results. Interestingly, over the range of operating conditions considered in this work, the specific wetted area is found to be simply a constant,

$$a_w = 0.5a \,. \tag{3.20}$$

The value of the heat loss, q''_{HL}, is experimentally determined and is diffusion tower specific. There was negligible heat loss for the heated air/ambient water case thus the heat loss flux term is taken to be zero. The heat loss for the heated air/heated water case is experimentally calibrated for various air mass fluxes. Figure 3-2 shows the calibration curve for the heated air/heated water heat loss flux for varying air mass flux.

To solve the three coupled equations for the humidity ratio, air temperature, and water temperature distributions in the diffusion tower, the following solution procedure is followed:

1. Specify the water mass flux, air mass flux, inlet water temperature, inlet air temperature, and inlet humidity ratio.
2. Guess a value of the exit water temperature.
3. Compute the exit humidity ratio, exit water temperature, and exit air temperature utilizing Equations 3.6, 3.10, and 3.14 until z reaches the height of the packed bed.
4. Compare the values of the calculated inlet water temperature and specified inlet water temperature. If they match, the analysis is complete. If they differ, repeat the procedure beginning from step 2.

Results and Discussion

Experiments were conducted to obtain data for the two different cases: heated air/ambient water and heated air/heated water. For both cases, the air mass flux was held constant at about 0.77 kg/m^2-s, 1.16 kg/m^2-s, and 1.55 kg/m^2-s while the liquid mass flux was varied between 0.6 kg/m^2-s to 1.3 kg/m^2-s. The height of the packed bed was held constant at 0.38 m. All experiments conducted were performed in a parameter space beneath the flooding curve for the packed bed. For the model analysis, the inlet water temperature, inlet air temperature, and inlet absolute humidity were all used to compute

the exit conditions. Comparisons between the predicted and measured exit conditions from the model are described next.

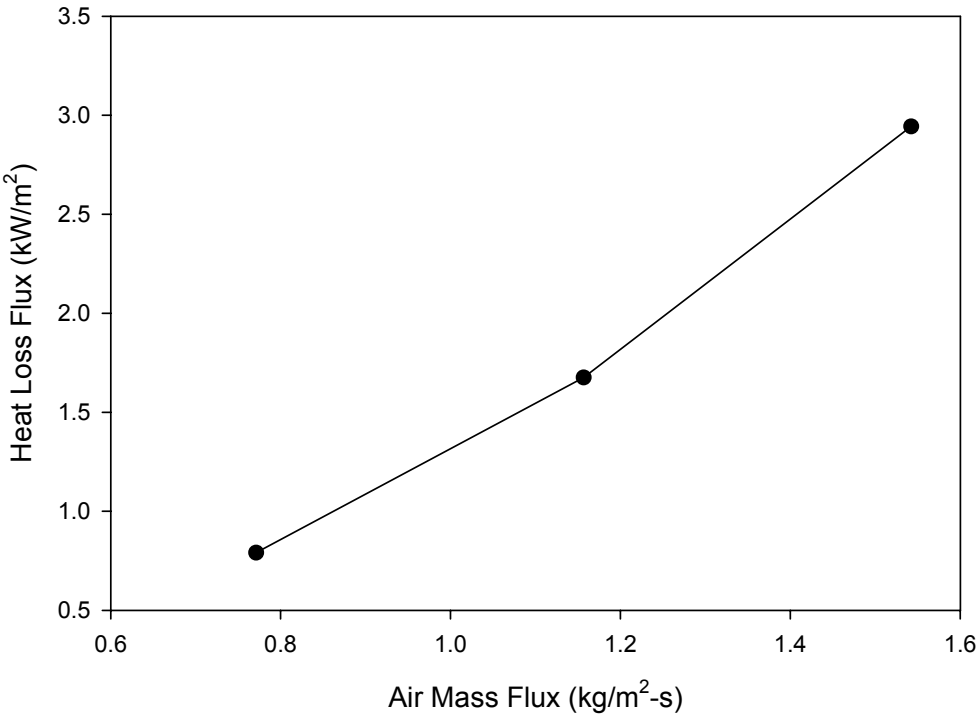

Figure 3-2. Calibration curve of the heat loss flux for the heated air/heated water case.

Case 1: Heated Air/Ambient Water

Six different data sets were recorded for the heated air/ambient water case. Two different data sets per air mass flux were taken to ensure the repeatability of the experiments. For all experiments, the inlet air, water, and humidity were held constant at about 60.9 °C, 25.2 °C, and 0.0060 respectively. Figures 3-3 to 3-5 show the comparison between the predicted exit values and the measured exit values. The comparison between the two is quite good. The exit absolute humidity and exit water temperature are predicted with fairly good accuracy while the exit air temperature is slightly underpredicted for all data sets.

From the data collected it can be seen that the heated air/ambient water case does not yield good production. The exit air temperature is approximately 25-26 °C for each value of the liquid mass flux as well as air mass flux, which indicates that the air is cooled to the temperature of the water. This is supported by the fact that the temperature difference of the exit water and exit air is nearly a constant 1-2 °C. Thus it is clear that reliance on heated air is inefficient because upon entering the tower the air is immediately cooled close to the water temperature. All of the energy is being used to heat up the water and as a result the mass transfer is poor. As the absolute humidity shows, there is no optimum value as the exit humidity is essentially constant. Further, the change in humidity from the inlet to the outlet essentially remains a constant at about 0.0125. This indicates that regardless of the diffusion tower liquid mass flux only a small fraction of water will be evaporated.

Figure 3-6(a-c) shows the repeatability of the six different experiments for the different flow conditions. As shown in the figures, the repeatability of the experiments is very good. However, the figures also elucidate the fact that the heated air/ambient water case is very inefficient. There is little variation between the values recorded for the six different experiments despite the different air and water mass fluxes used in the experimental measurements. For example, consider the exit air temperature shown in Fig. 3-6(a). For the three values of air mass flux the exit air temperature remains almost a constant despite the varying liquid mass flux. The exit water temperature and the exit humidity also demonstrate similar behavior. The process will exhibit the same behavior despite the operating conditions chosen.

(a)

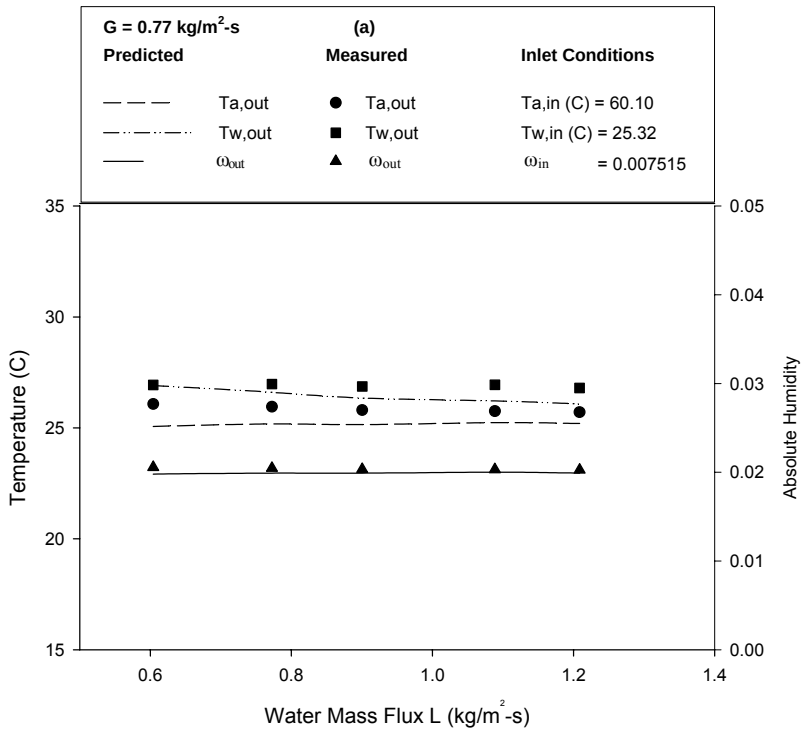

(b)

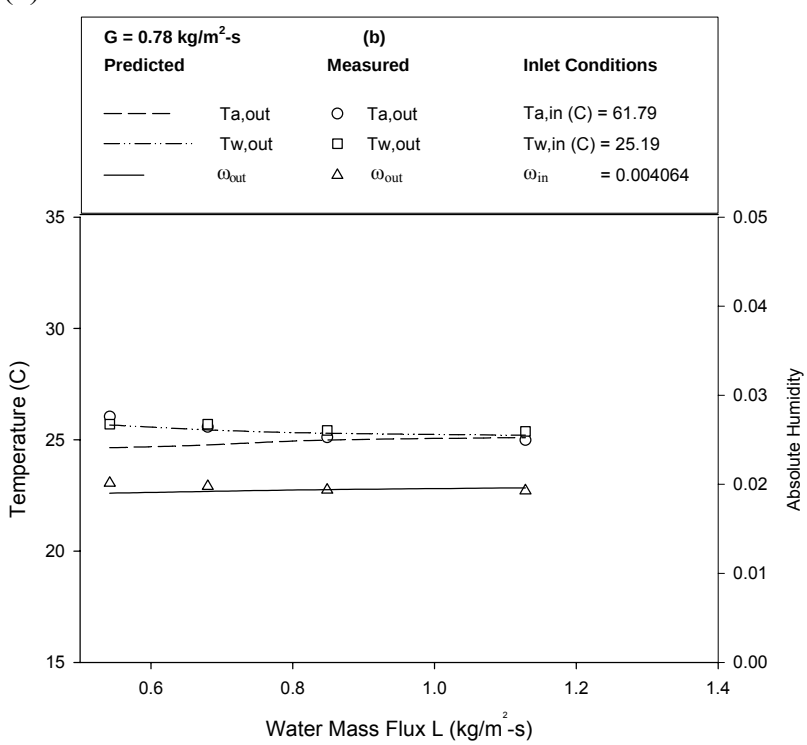

Figure 3-3. Comparison of predicted and measured exit temperatures and humidity for similar air mass flux G = 0.77 kg/m^2-s: a) Set 1 b) Set 2.

(a)

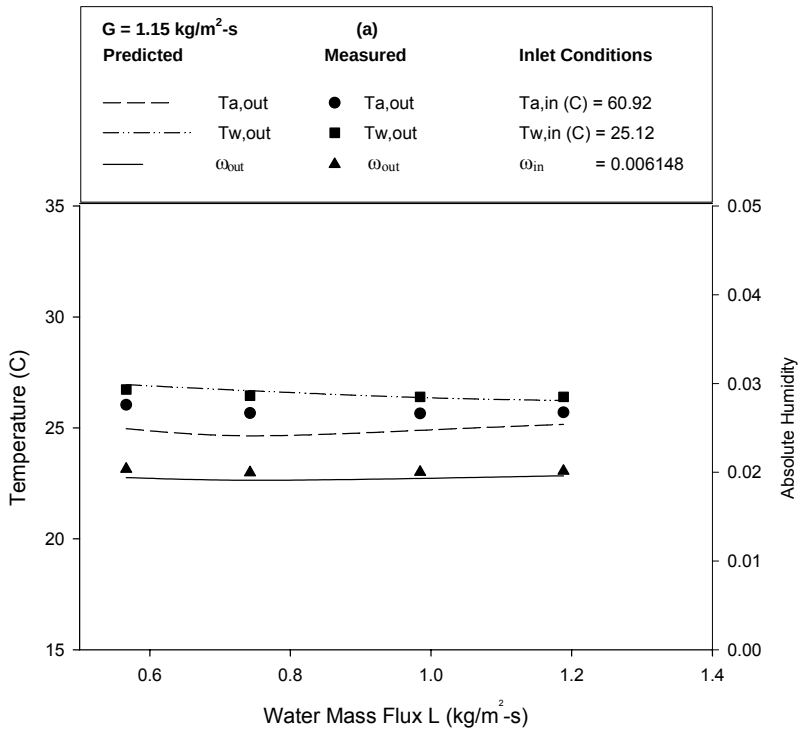

(b)

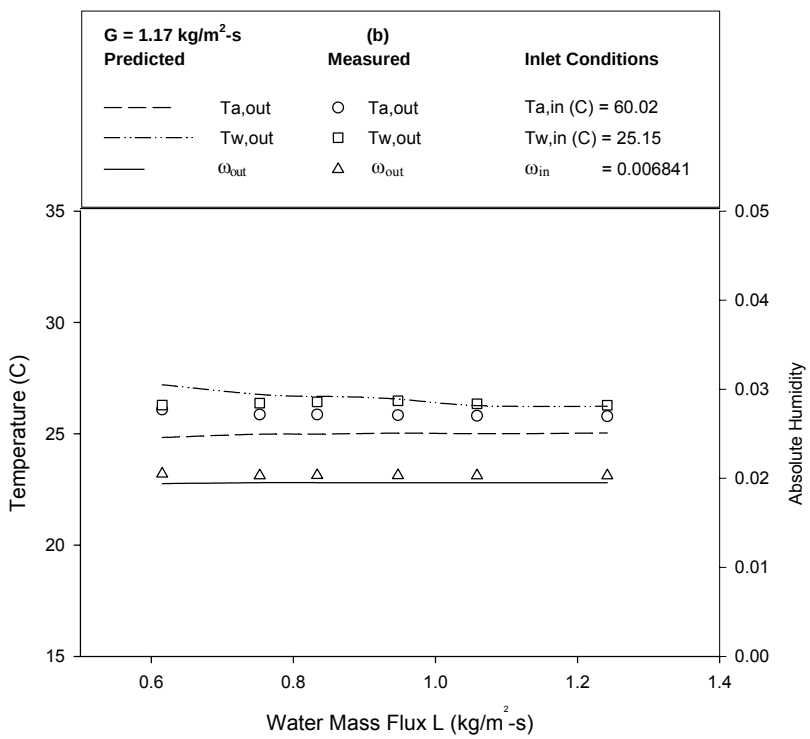

Figure 3-4. Comparison of predicted and measured exit temperatures and humidity for similar air mass flux G = 1.15 kg/m^2-s: a) Set 1 b) Set 2.

(a)

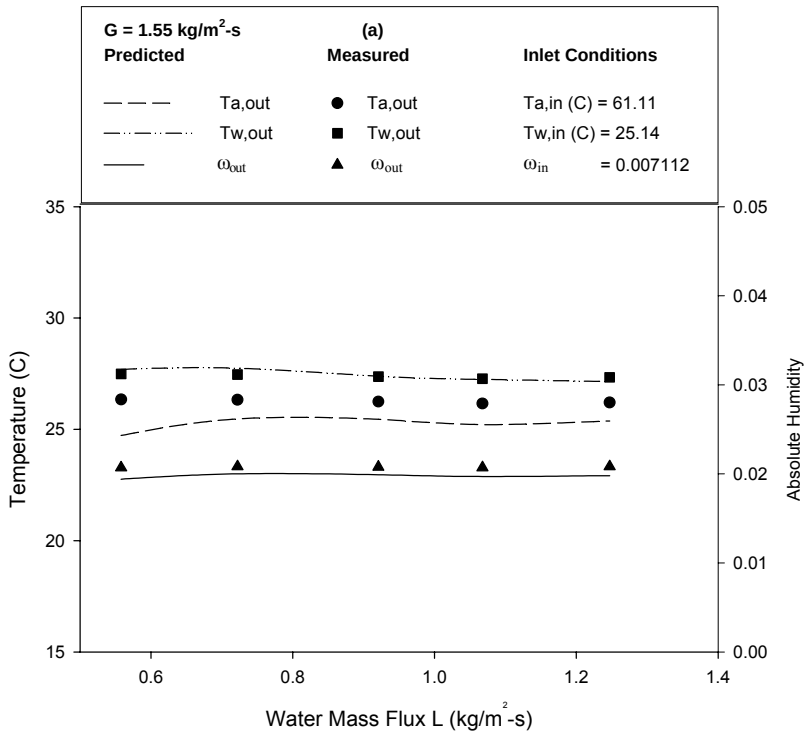

(b)

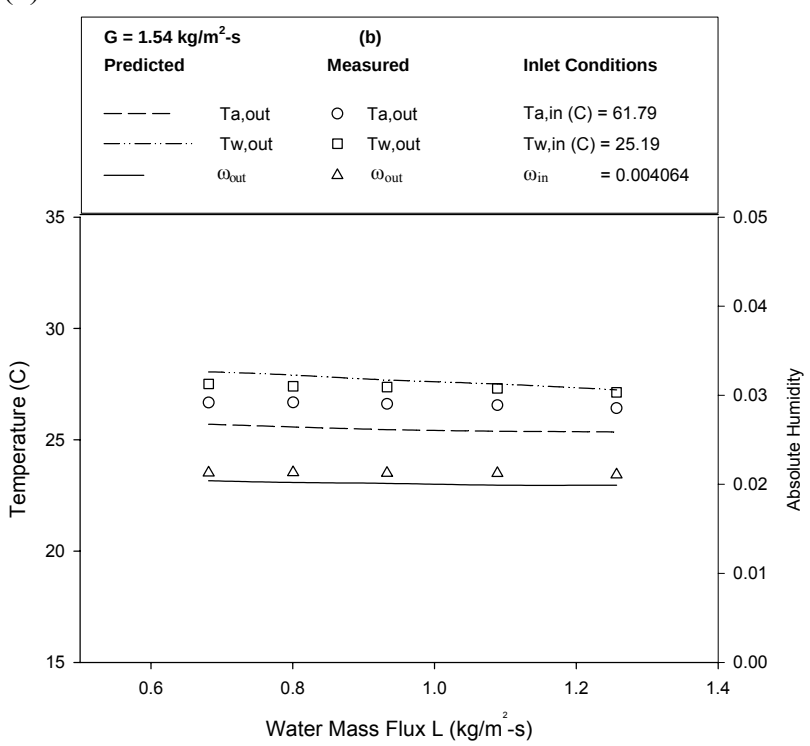

Figure 3-5. Comparison of predicted and measured exit temperatures and humidity for similar air mass flux G = 1.55 kg/m^2-s: a) Set 1 b) Set 2.

Details of the experimental data can be found in Appendix B.

Case 2: Heated Air/Heated Water

As in the previous case, six different data sets were taken, two for each different air mass flux. For all six experiments the inlet air temperature, water temperature, and humidity were held constant at about 60.9 °C, 60.6 °C, and 0.0077 respectively. Figures 3-7 to 3-9 show the comparison between the predicted and measured exit temperatures and humidity. For all sets of data the exit water temperature and exit humidity are predicted with considerable accuracy. The air temperature is slightly overpredicted in all cases.

(a)

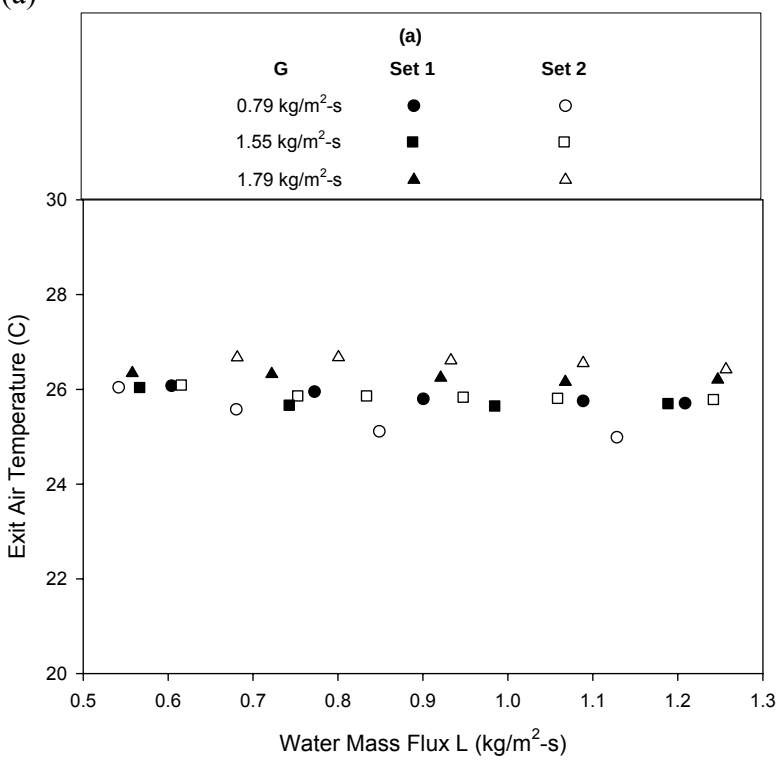

Figure 3-6. Repeatability of different experiments for different exit parameters: a) Exit air temperature, b) Exit water temperature, c) Exit absolute humidity.

(b)

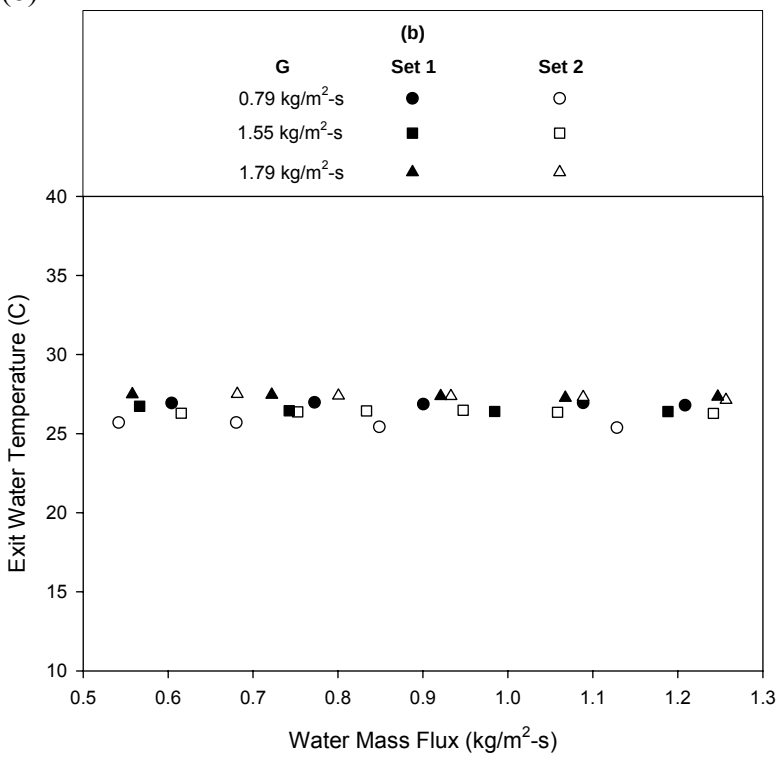

(c)

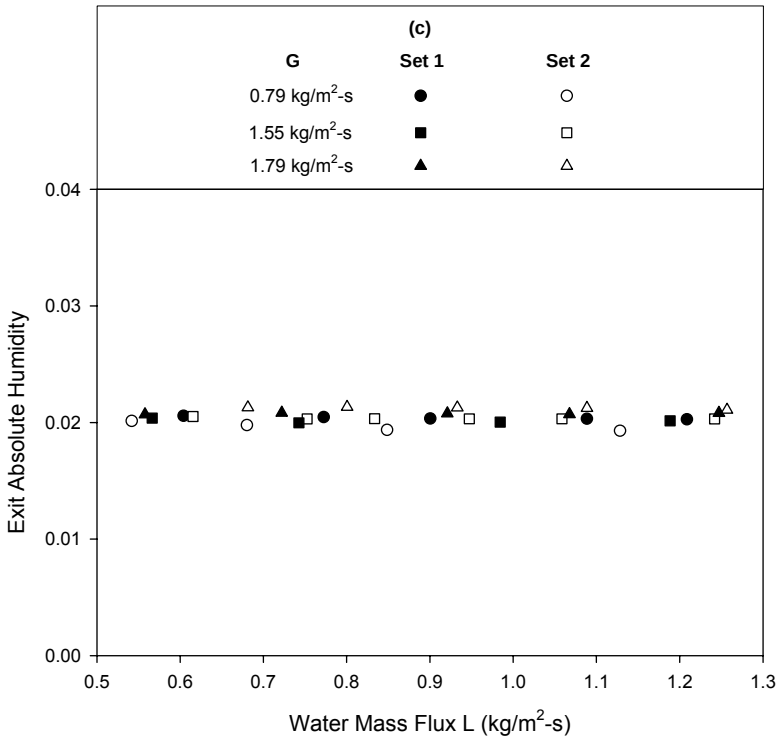

Figure 3-6. Continued.

(a)

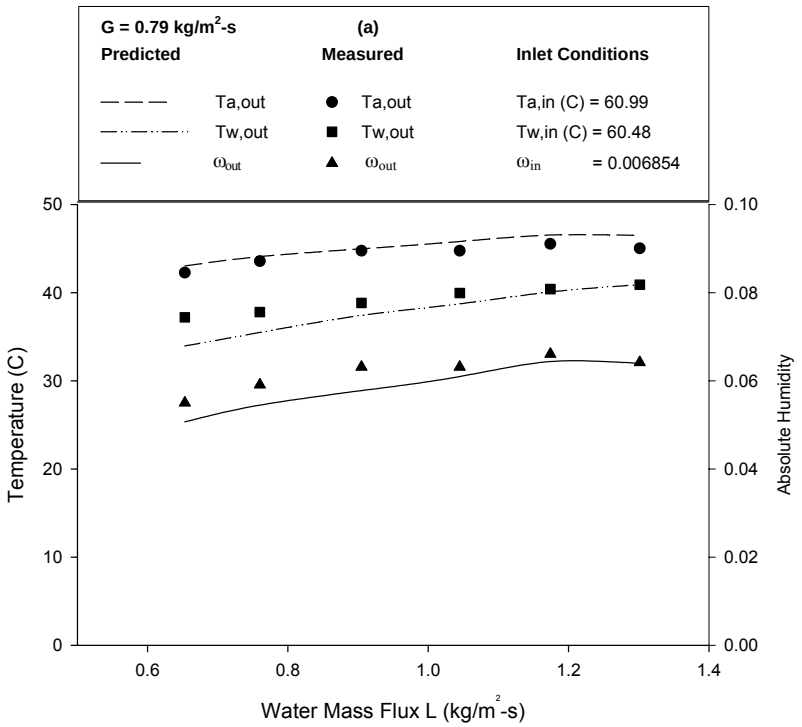

(b)

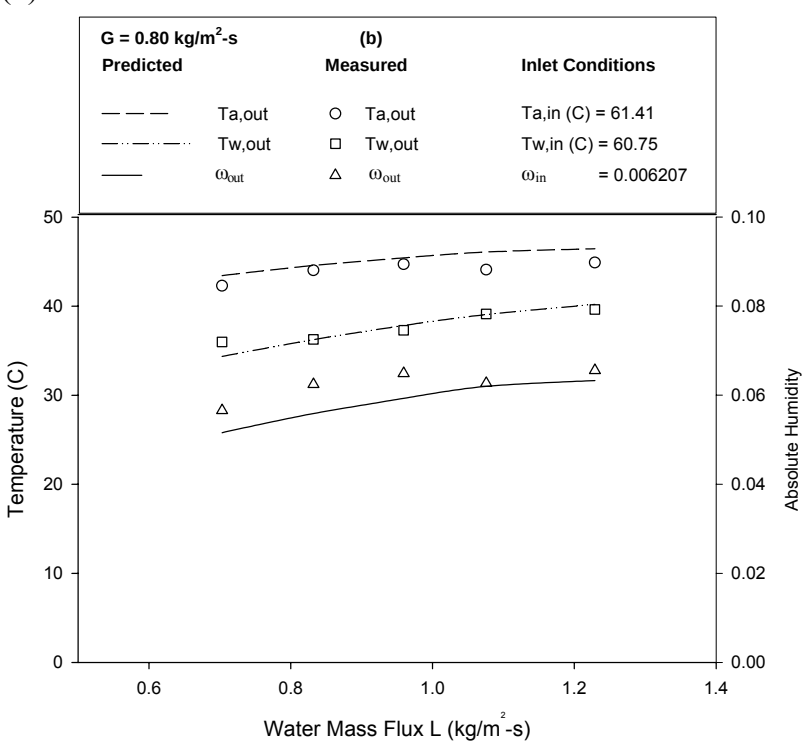

Figure 3-7. Comparison of predicted and measured exit temperatures and humidity for similar air mass flux G = 0.79 kg/m^2-s: a) Set 1 b) Set 2.

(a)

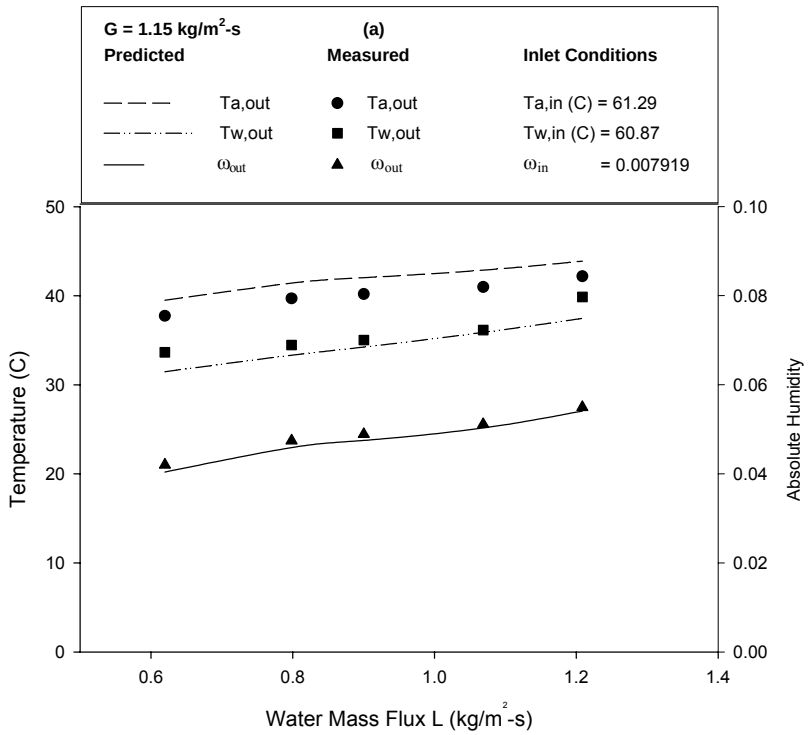

(b)

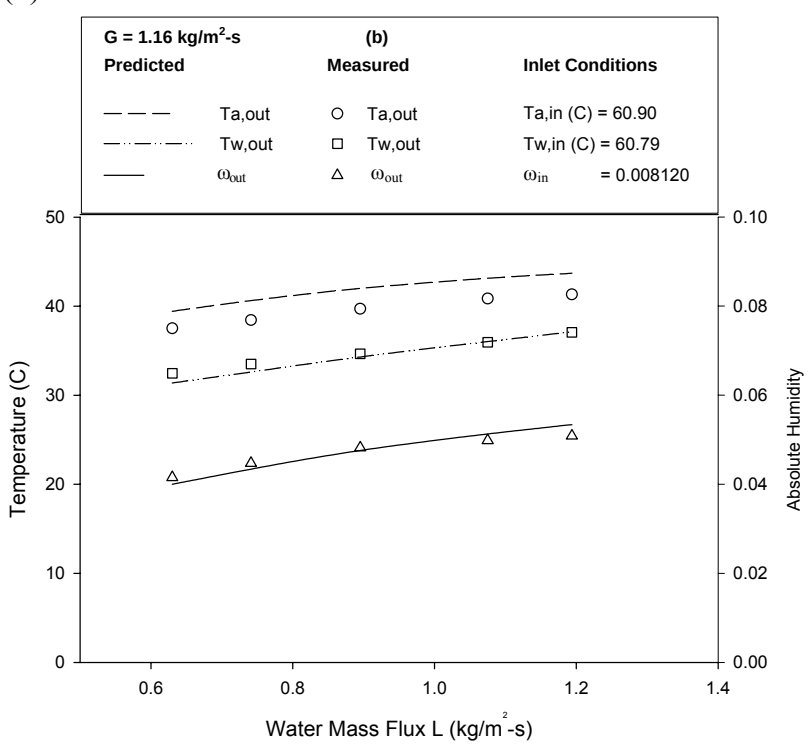

Figure 3-8. Comparison of predicted and measured exit temperatures and humidity for similar air mass flux G = 1.15 kg/m^2-s: a) Set 1 b) Set 2.

(a)

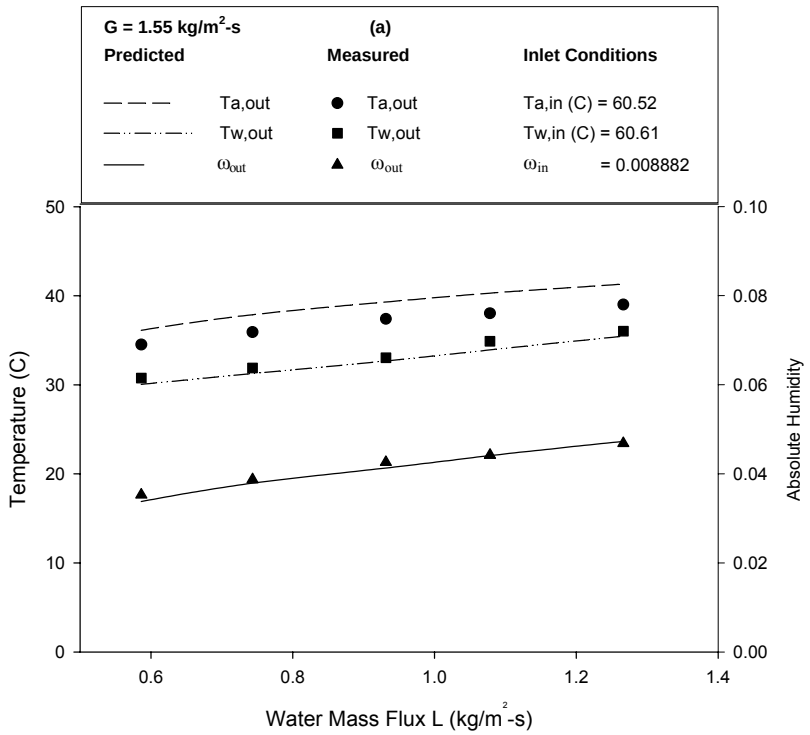

(b)

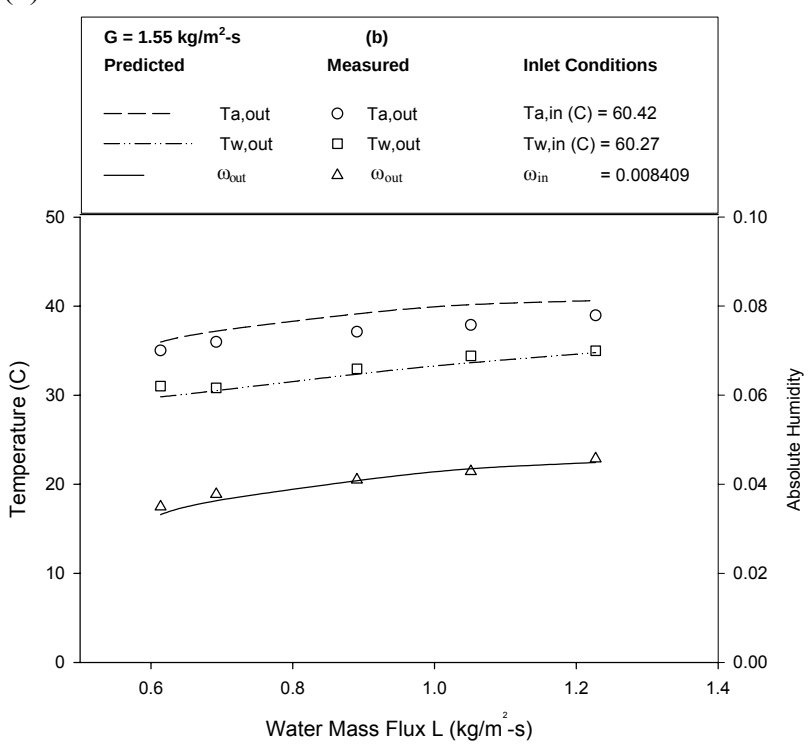

Figure 3-9. Comparison of predicted and measured exit temperatures and humidity for similar air mass flux G = 1.55 kg/m^2-s: a) Set 1 b) Set 2.

For all air mass fluxes studied, the exit air temperature and exit water temperature increase with increasing water mass flux. As the liquid mass flux increases the exit humidity also increases due to the increase in the amount of liquid available to evaporate.

Figures 3-10(a-c) demonstrates the repeatability of the six experiments for the heated air/heated water case. As shown in the figures the repeatability for all of the experiments is quite reasonable. These figures show that at the lower air mass flux the maximum exit humidity is obtained. It is also interesting that both the exit air temperature and exit water temperature decrease with increasing air mass flux. This suggests that the residence time plays a key role in the heat and mass transfer. A decrease in residence time implies that there is less time for heat and mass transfer to occur thereby explaining the decreased temperatures as well as humidity with increasing air mass flux. As demonstrated, the theoretical model developed is obviously a good design tool that can be utilized to achieve the desired production rate.

Details of the experimental data collected for the heated air heated water case can be viewed in Appendix C.

(a)

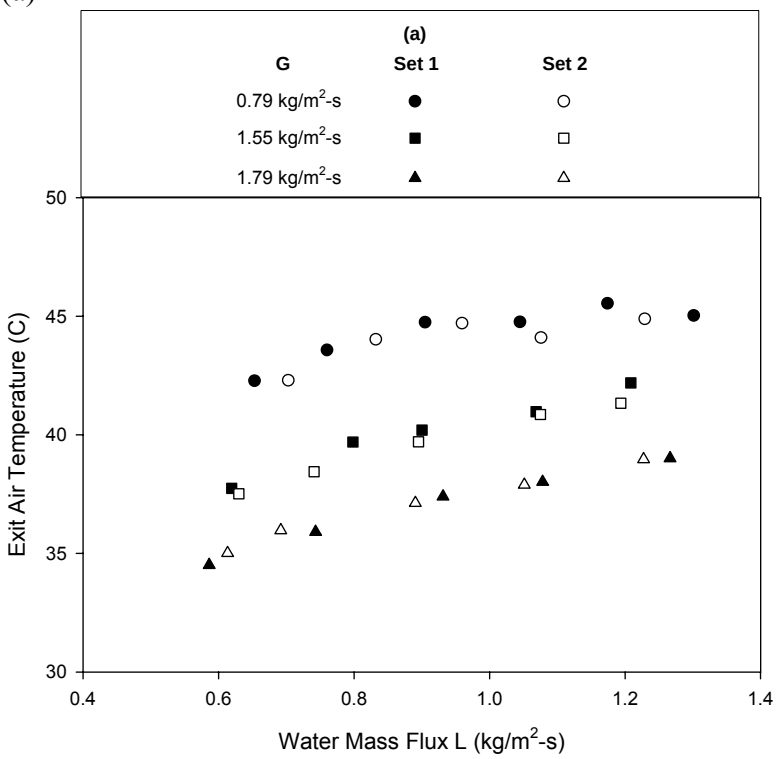

(b)

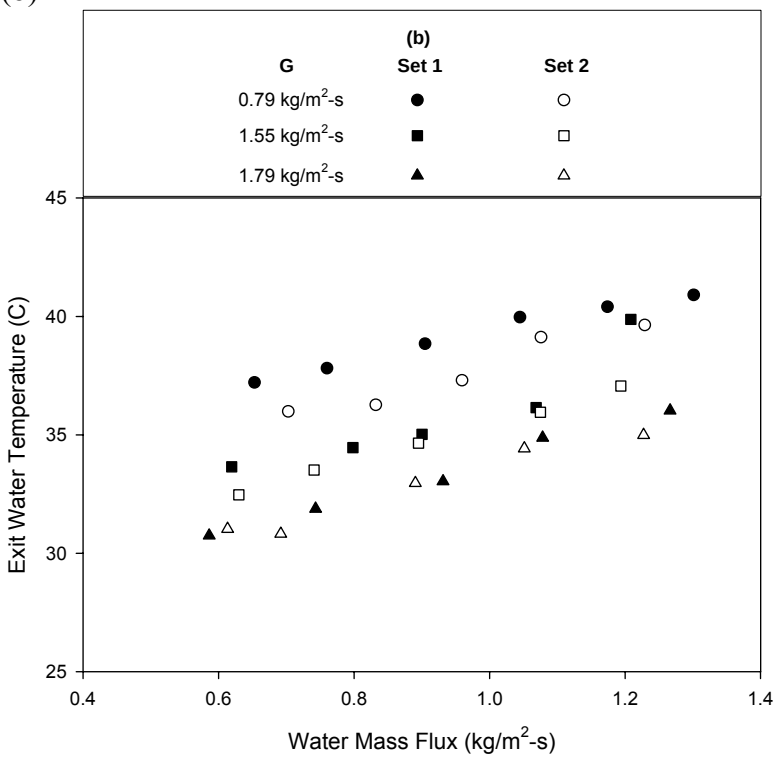

Figure 3-10.Repeatability of experiments for different exit parameters: a) Exit air temperature, b) Exit water temperature, c) Exit absolute humidity.

(c)

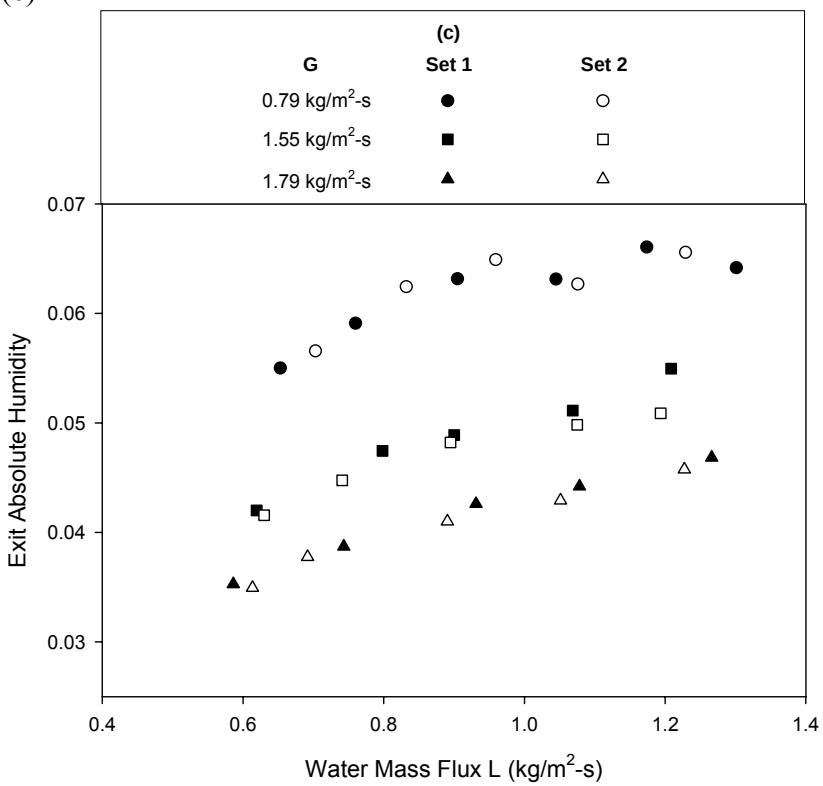

Figure 3-10. Continued.

CHAPTER 4
PARAMETRIC ANALYSIS

The previous chapters have focused on the experimental facility, data collection, the heat and mass transfer model, and comparisons of the predicted and measured data. It has been shown that the DDD process has good performance for the heated air/heated water case, while the heated air/ambient water case is inefficient. In order to fully explore the feasibility of the heated air/heated water DDD process a parametric analysis is considered. This chapter details the parametric analysis including the methodology, analysis of results, and comparisons between several different DDD processes. At the end of the chapter an economic analysis of the DDD facility for coupling with an industrial plant that produces large quantities of waste heat in air is explored.

Parametric Analysis of Heated Air/Heated Water DDD Process

The heat and mass transfer model described in Chapter 3 is used to model the heated air/heated water DDD process. The assumptions made in this analysis are:

1. There is no heat lost to the surrounding environment.
2. The only energy consumed is the pumping power required to pump the air and water through the system.
3. The air/vapor mixture is treated as a perfect gas.
4. Changes in potential and kinetic energy are considered to be negligible.
5. The process operates at steady-state conditions.

Equations 3.6, 3.10, and 3.14 are used to evaluate the absolute humidity, water temperature, and air temperature respectively through the diffusion tower. The heat and

mass transfer analogy is used to evaluate the heat transfer coefficients and Onda's correlation is used to evaluate the mass transfer coefficients assuming a constant wetted area.

In order to fully explore the bounds of the heated air/heated water DDD process the energy consumption must be evaluated and certain parameters are needed to effectively assess the process. The fresh water production rate is computed from,

$$m_{fw} = GA(\omega_{out} - \omega_{in}), \tag{4.1}$$

where the subscripts fw, in, and out refer to the fresh water and diffusion tower inlet and outlet respectively. It should be noted that it is assumed that the carrier air circulates in a closed loop and the inlet humidity to the diffusion tower is the outlet humidity from the condenser.

The major energy consumption of the process is assumed to be the pumping power required to pump the air and water through the system. The pumping power required for the diffusion tower gas is

$$E_G = V_G \Delta P_G = \frac{m_G}{\rho_G} \Delta P_G = \frac{GA}{\rho_G} \Delta P_G \ . \tag{4.2}$$

In order to evaluate the pressure drop on the gas side a correlation provided by the packing material company, Lantec, is used. The pressure drop, ΔP_G, across the HD Q-PAC packed bed is computed from,

$$\frac{\Delta P_G}{z} = \frac{G^2}{\rho_G}[0.0354 + 654.48(\frac{L}{\rho_l})^2 + 1.176 \times 10^7 (\frac{L}{\rho_l})^4 \frac{G^4}{\rho_G^2}], \tag{4.3}$$

where ΔP_G is the pressure drop across the packed bed (kPa) and z is the height of the tower. The validity of the correlation was explored by Li [15], and it has excellent agreement with the experimental data.

The pumping power required for the diffusion tower liquid is calculated as,

$$E_L = \frac{m_L}{\rho_L} \Delta P_L = LAgH \ . \tag{4.4}$$

Thus the total pumping power is calculated as,

$$E_{total} = E_L + E_G \ . \tag{4.5}$$

The energy consumption rate per unit of fresh water production is defined as,

$$E_{fw} = \frac{E_{total}}{m_{fw}} . \tag{4.6}$$

The fresh water production rate and energy consumption rate are two important parameters that characterize the performance of the DDD process. The fresh water production rate characterizes the quantity of fresh water produced at a given set of operating conditions while the energy consumption rate denotes how much energy is consumed per unit of fresh water produced. The two values are important in finding the optimal operating conditions. An ideal DDD process would have a high fresh water production rate and a low energy consumption rate.

Heated Air/Heated Water Results and Discussion

Using the analysis described above and the theory discussed in Chapter 3, a parametric analysis is performed to determine the effects of certain operating variables on the performance of the heated air/heated water process. In performing the analysis, the air inlet temperature, water inlet temperature, specific packing area, diameter of the packing material, and inlet humidity ratio were all held constant at 60° C, 60° C, 267

m^2/m^3, 0.018 m, and 5.25% respectively. Nine different values of the inlet feedwater mass flux, L, were considered 0.15, 0.25, 0.5, 0.75, 1.20, 1.55, 2.0, 2.5, 3.0 kg/m^2-s. The inlet air mass flux, G, was varied continuously from 0.04 to 23.2 kg/m^2-s for each inlet feedwater flux. For each air mass flux, the maximum absolute humidity was determined, and the tower height, air exit temperature, and water exit temperature were recorded. All calculations were performed in a parameter space below the flooding curve of the packing material.

Figure 4-1 depicts the tower height as a function of the inlet air mass flux. The tower height reported is the computed tower height required to achieve the maximum exit absolute humidity. For all inlet liquid mass fluxes, the tower height decreases with increasing inlet air mass flux. This is important because as the air mass flux increases,

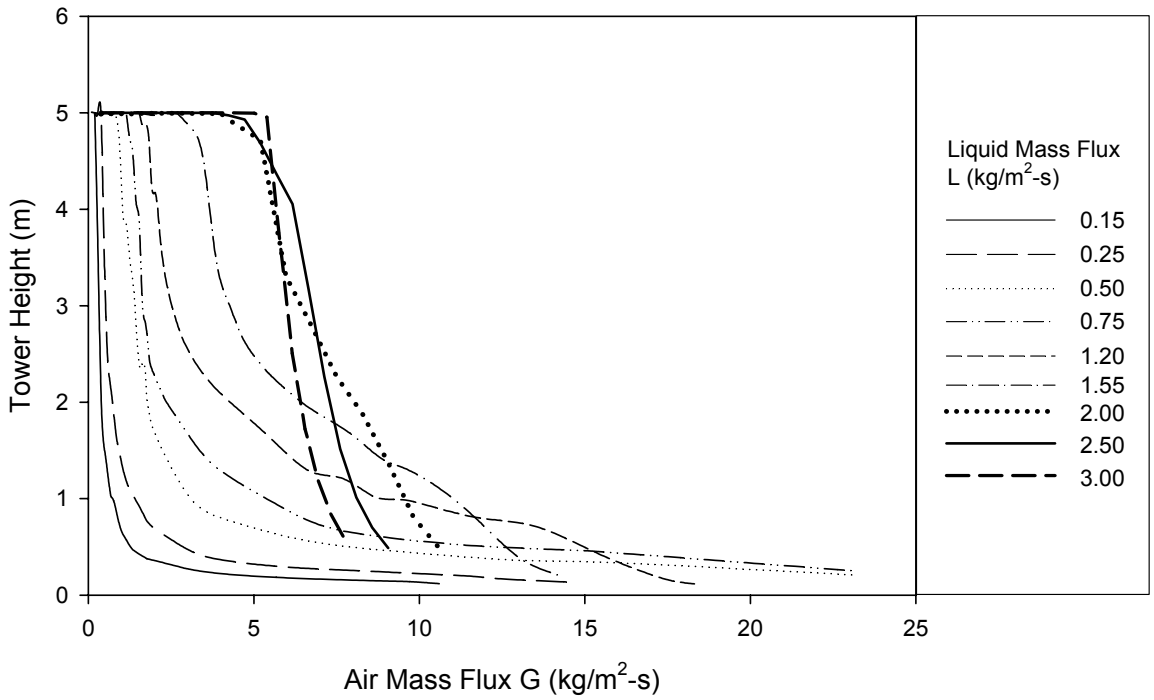

Figure 4-1. Tower height at the maximum exit absolute humidity as a function of the inlet air mass flux G.

the tower height decreases which translates to less required materials and thus reduced cost. However, as the air mass flux increases the power required to pump the air also increases. It should be noted that the tower height for high liquid mass flux and low air mass flux was restricted to values less than 5 m. This is to ensure that the tower heights considered are realistic.

Figure 4-2 shows the exit air temperature with varying air mass flux. The exit air temperature decreases with increasing air mass flux until it reaches a minimum value then increases. It is also worthy to note that the highest exit air temperatures are realized when the air mass flux is low.

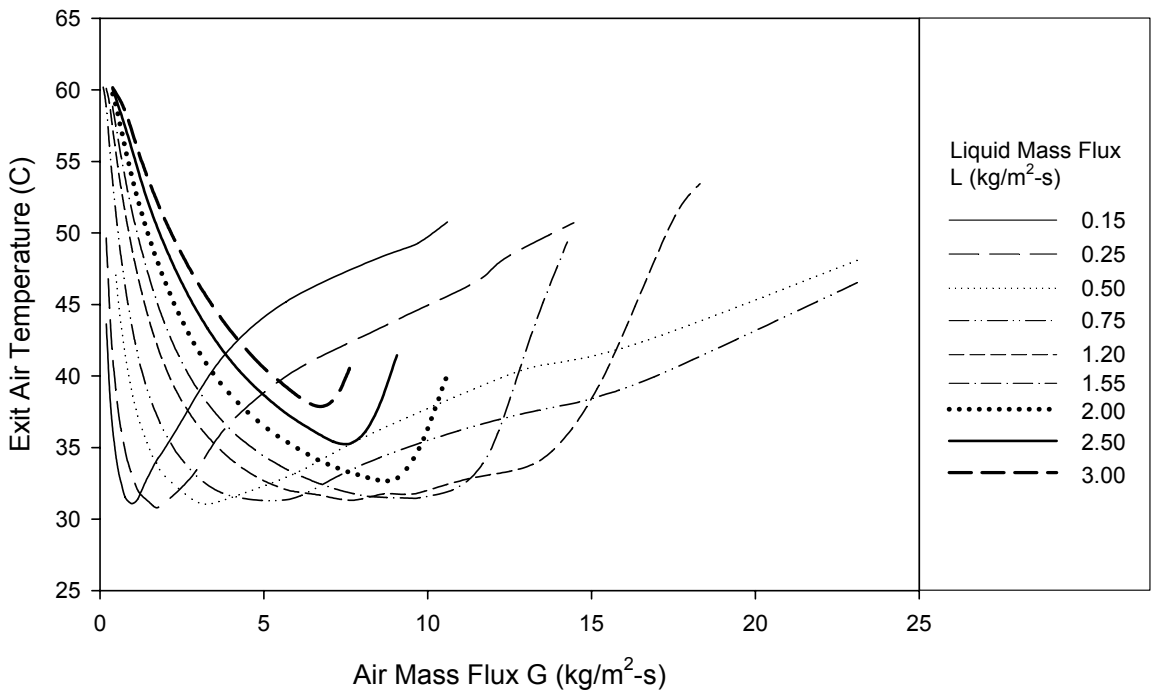

Figure 4-2. Exit air temperature at maximum absolute humidity as a function of the air mass flux.

Figure 4-3 depicts the maximum exit absolute humidity as a function of air mass flux for varying liquid mass flux values. For all liquid mass flux values, the exit humidity decreases with increasing air mass flux. The maximum exit humidity is

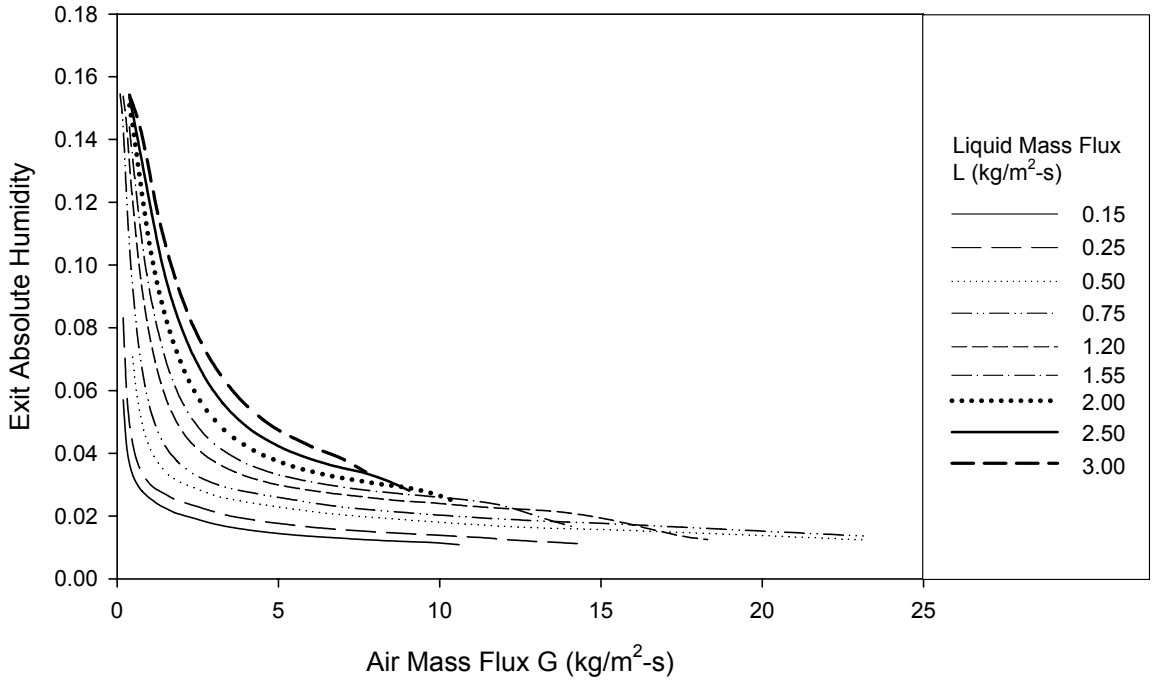

Figure 4-3. Maximum exit absolute humidity with varying air mass flux.

achieved with the higher liquid mass fluxes and can be attributed to the fact that the heat capacity of the water is large with larger mass fluxes, and the water temperature will not decrease as much with a given amount of evaporation. Thus as the liquid mass flux decreases the exit absolute humidity decreases as well. The maximum exit humidity is realized for low values of the air mass flux. It is important to note that the maximum exit air temperature and maximum humidity for all liquid mass fluxes are achieved for values of the air mass flux less than about 2.00 kg/m^2-s. While the exit air temperature and exit absolute humidity are maximum at low air mass flux, this does not imply that the fresh water production will also be high.

The fresh water production is an important parameter in evaluating the economy of the process. Figure 4-4 shows the fresh water production flux with varying air mass flux. For each value of the liquid mass flux the fresh water production flux increases until it

reaches an optimum condition. This is important because it indicates that for every liquid mass flux there is a value of the air mass flux that can produce the maximum amount of fresh water. It is also important to notice that as the liquid mass flux increases, the fresh water production flux increases. Thus a higher production can be achieved at higher liquid mass flux. Interestingly, for all liquid mass flux the maximum fresh water production does not occur below 2.00 kg/m^2-s where the maximum exit humidity is realized.

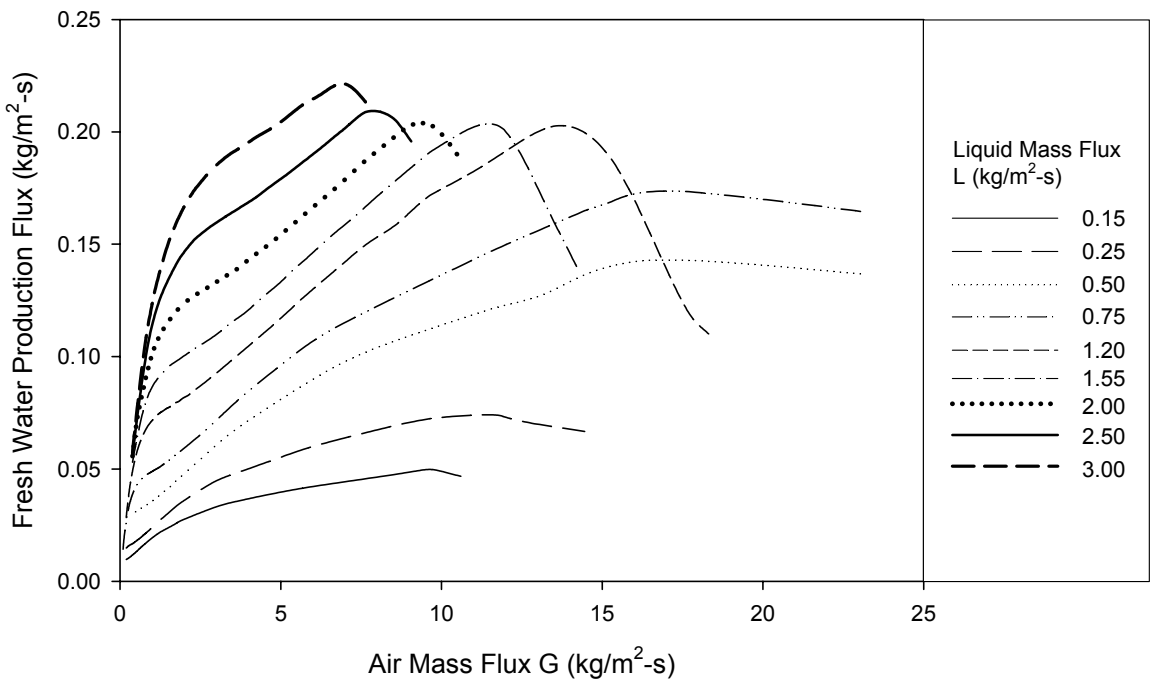

Figure 4-4. Fresh water production flux with varying air mass flux.

The energy consumption rate is also an important parameter in evaluating the economy of the DDD process. Figure 4-5(a-b) shows the energy consumption rate for the diffusion tower with varying air mass flux for the different values of the liquid mass flux. Figure 4-5(a) shows the full range of air mass flux while Figure 4-5(b) shows a smaller range. For all values of liquid mass flux, the energy consumption rate increases

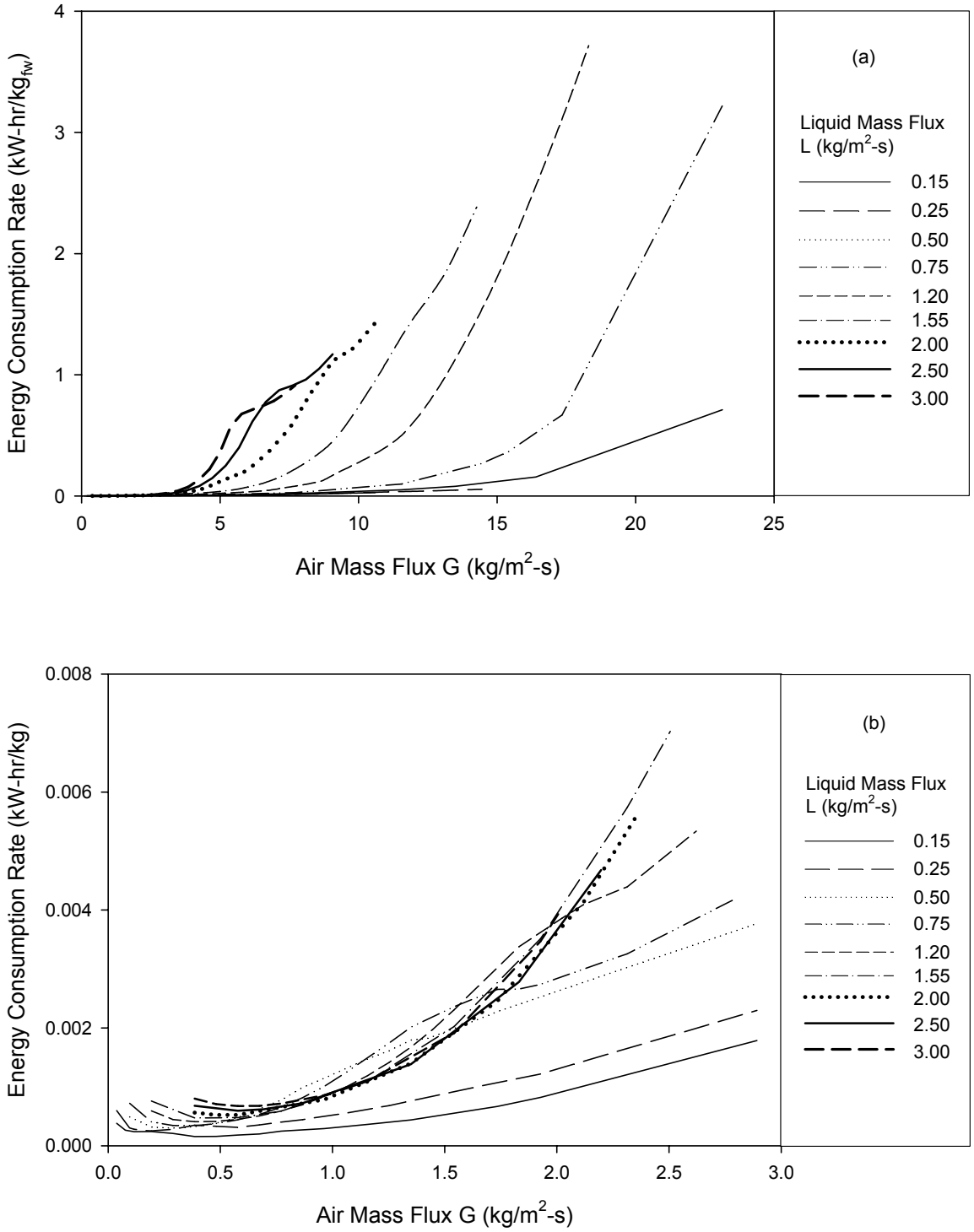

Figure 4-5. Diffusion tower energy consumption rate (a) with varying air mass flux (b) for low air mass flux.

with increasing air mass flux. The higher the air mass flux, the more pumping power required to drive the process. As the graphs reveal there is a minimum energy

consumption rate for each liquid mass flux. Beyond that optimum value, the energy consumption steadily increases. From Figure 4-5(a) it can be seen that operating at higher air mass flux is impractical due to the high energy consumption rate. Li et al. [11] reported that the ideal operating condition in the condenser is for air mass flux below 1.5 kg/m^2-s to ensure low energy consumption. Figure 4-5(b) reiterates this condition for the diffusion tower. Below an air mass flux of 1.5 kg/m^2-s, the energy consumption is low.

Figure 4-6 shows the fresh water production efficiency versus the air mass flux for varying liquid mass flux. The fresh water production efficiency increases with increasing air mass flux until it reaches a maximum condition, and then it steadily decreases. As the liquid mass flux increases the maximum fresh water production efficiency decreases. The maximum efficiency occurs for low liquid mass flux while the maximum fresh water production occurs for high liquid mass flux. An optimal operating condition is one that has high fresh water production and low energy consumption.

Comparison of Different DDD Processes

Next the heated air/heated water DDD process will be compared against other DDD configurations. The heated air/heated water DDD process will first be compared against the process described by Klausner et al. [16], heated water/ambient air for a 60 °C water inlet. The process will then be compared against the heated air/heated water DDD process with Q-PAC, a packed bed with a smaller specific area and lower pressure drop.

Heated Water/Ambient Air at 60 °C

In this analysis the heated air/heated water DDD process is compared against the heated water/ambient air DDD process described by Klausner et al. [16]. In performing the analysis of the heated air/heated water the analysis described in Chapter 3 is used

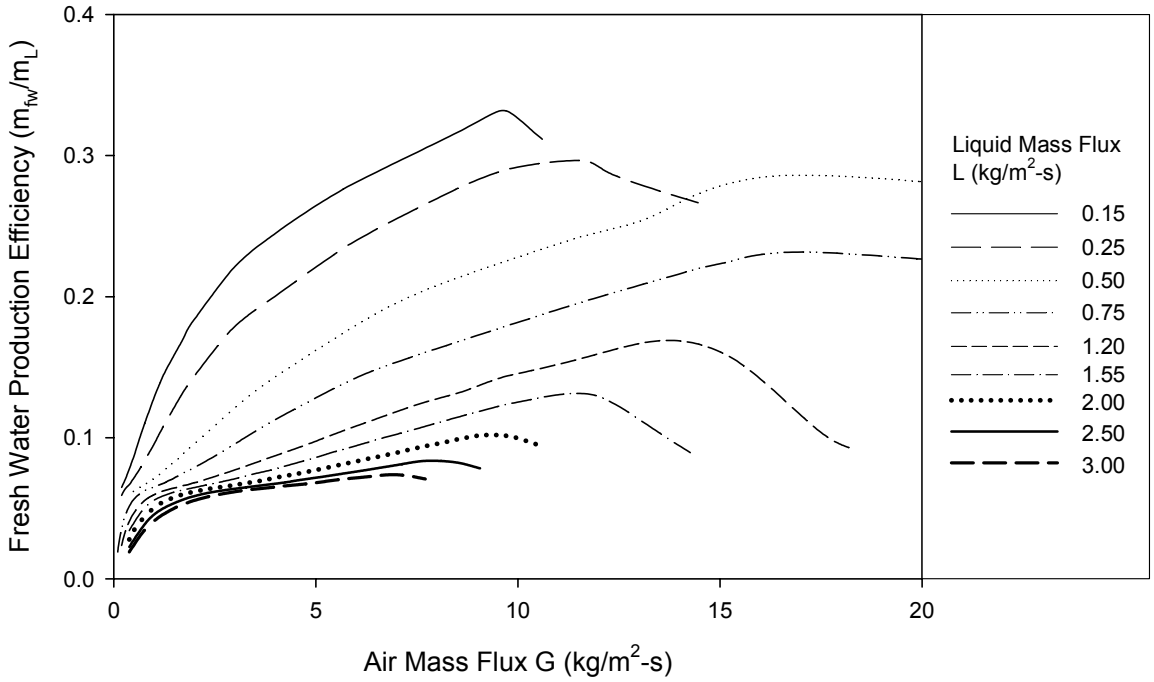

Figure 4-6. Fresh water production efficiency with varying air mass flux realized for the lower air and liquid mass fluxes.

with the air inlet temperature, water inlet temperature, specific packing area, diameter of the packing material, and inlet absolute humidity held constant at 60° C, 60° C, 267 m^2/m^3, 0.018 m, and 0.0065 respectively. The values obtained for the heated water/ambient air case are calculated using the model proposed by Klausner et al. [16] where the inlet water temperature, inlet air temperature, inlet humidity ratio, specific area, and diameter of the packing are held at 60° C, 26° C, 0.023, 267 m^2/m^3, and 0.018 m respectively. To obtain the predictions for comparison calculations were run for nine different liquid mass fluxes: 0.15, 0.25, 0.5, 0.75, 1.20, 1.55, 2.0, 2.5, 3.0 kg/m^2-s. For each liquid mass flux, the gas mass flux was varied. For each liquid mass flux, the minimum energy consumption rate was recorded over the range of air mass flux. The values of the fresh water production flux, and fresh water production efficiency reported

are those corresponding to the point of minimum energy consumption. Figures 4-7 and 4-8 show the fresh water production flux, energy consumption rate, and fresh water production efficiency for the two different configurations.

Figure 4-7 shows the fresh water production efficiency and energy consumption rate with varying liquid mass flux for both of the processes. The energy consumption rate for both shows little difference for liquid mass fluxes greater than about 1.3 kg/m^2-s. However at low mass flux the heated water/ambient air case has a considerably less energy consumption rate. The fresh water production efficiency of the heated air/heated water process is greater for all values of liquid mass flux, although at large liquid mass flux the difference is not significant. It should be noted that when comparing the two configurations there is more thermal energy input for the heated air/heated water case than the heated water/ambient air case, and the energy consumption rate only reflects the electrical energy consumed.

Figure 4-8 shows the fresh water production flux and energy consumption rate for varying liquid mass flux for both processes. It is observed that the heated air/heated water process has a greater fresh water production flux for all values of the liquid mass fluxes considered. However at low liquid mass flux, the energy consumption rate is higher for the heated air/heated water configuration. Thus the decision to use one process over the other depends upon the source of waste heat and operating conditions.

This comparison reveals that for higher liquid flow rates the heated air/heated water case is equally comparable in energy consumption rate but has a higher fresh water production efficiency and fresh water production flux. On a small scale, this equates to a

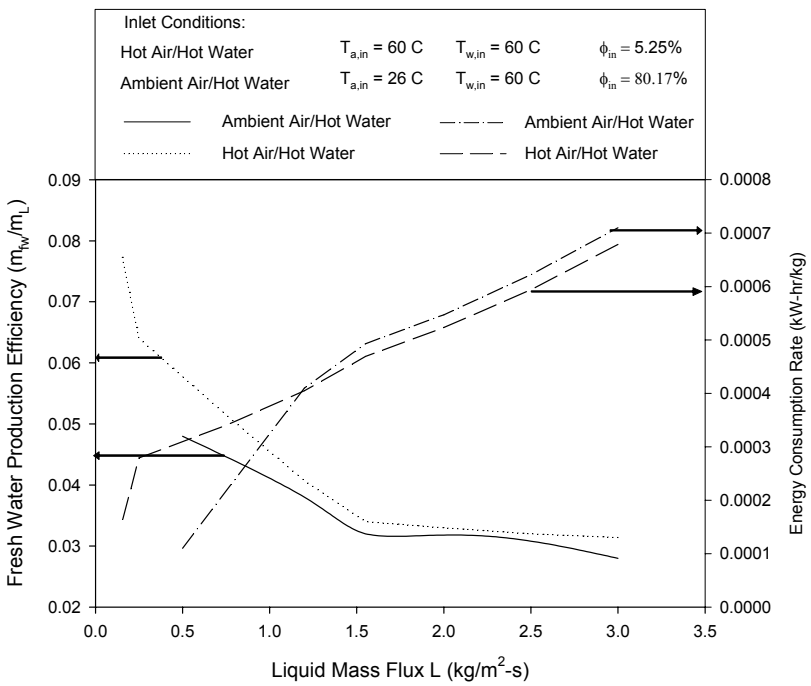

Figure 4-7. Fresh water production efficiency and energy consumption rate for varying liquid mass flux for 60 °C inlet conditions.

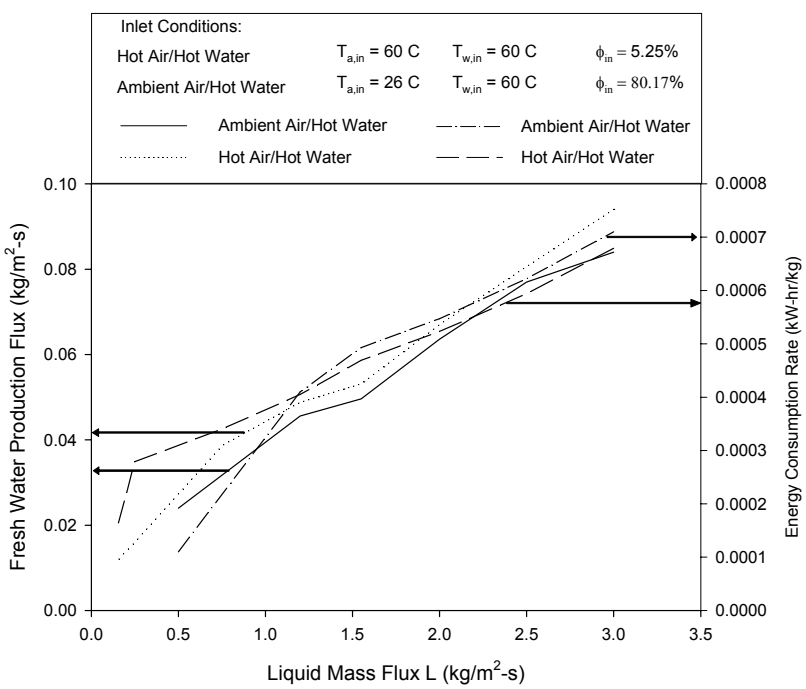

Figure 4-8. Fresh water production flux and energy consumption rate for varying liquid mass flux for 60 °C inlet conditions.

smaller tower size by utilizing the heated air/heated water DDD process. Less tower height is required for the heated air/heated water process in order to generate the same amount of fresh water produced in the heated water/ambient process. This translates to lower production cost and less space required.

Heated Air/Heated Water using Q-PAC

For the next analysis two different types of packed bed are used with the heated air/heated water process. The theoretical model proposed in Chapter 3 is used to calculate the parameters, however a different wetted specific area is used. A modified Onda's correlation, which is found in Appendix A, is used for the mass transfer coefficients and the wetted specific area for both configurations. HD Q-PAC, the packing material described in Chapter 2 and used in the experimental facility, is compared with Q-PAC. The Q-PAC material is also produced by Lantec and is manufactured to have lower pressure drop, reduced incidence of fouling, and flooding at higher air mass flow rates giving it a wider range of operation. Lantec supplied the gas side pressure drop, ΔP_G (kPa), across the Q-PAC packed bed as

$$\frac{\Delta P_G}{z} = \frac{G^2}{\rho_G}[0.0078 + 1.3788(\frac{L}{\rho_l}) + 0.30715(\frac{L}{\rho_l})^2 \frac{G^4}{\rho_G^2}], \tag{4.7}$$

Figures 4-9 and 4-10 show the fresh water production, fresh water efficiency, and energy consumption of the heated air/heated water process for the two configurations. Again the computations shown in the graph correspond to the points of minimum energy consumption rate for each liquid mass flux. Figure 4-9 shows the fresh water production efficiency and energy consumption rate with varying liquid mass flux. The Q-PAC packed bed configuration is obviously much more energy efficient than the HD Q-PAC configuration. As the liquid mass flux increases the variation in the energy consumption

rate of the two configurations increases. There is little variation in the fresh water production efficiency, however the Q-PAC appears to have a slightly better fresh water production efficiency for all values of the liquid mass flux explored.

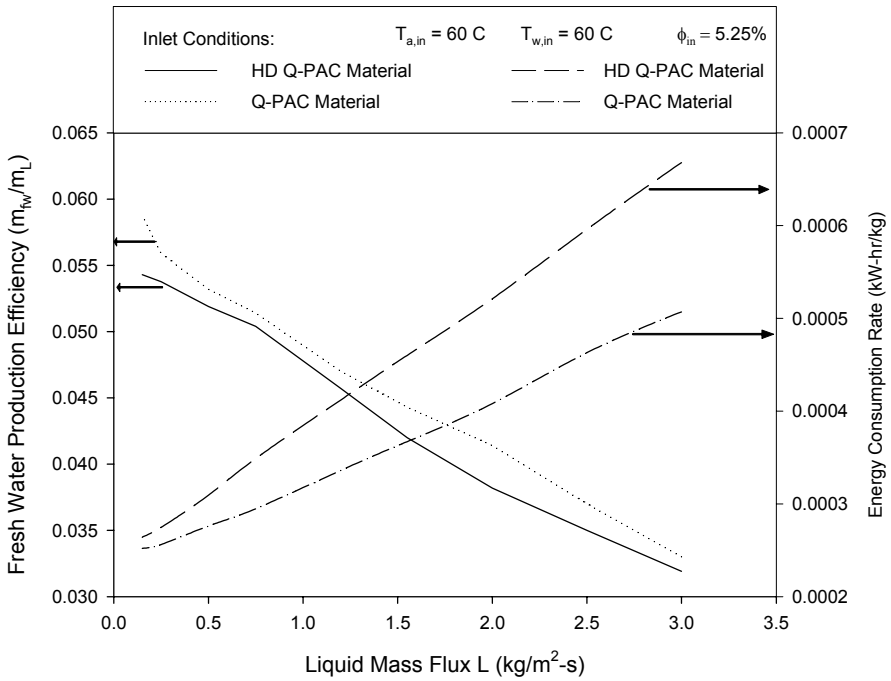

Figure 4-9. Fresh water production flux and energy consumption rate for varying liquid mass flux for HD Q-PAC and Q-PAC packed bed.

Figure 4-10 shows the variation in the fresh water production flux and energy consumption rate for varying liquid mass flux. There is very little variation in the fresh water production flux between the HD Q-PAC and Q-PAC packed bed configurations. However, at high liquid mass flux, the Q-PAC appears to have a slightly higher fresh water production flux. Despite the minimal difference in fresh water production between the two beds, the energy consumption rate remains the key difference. Figure 4-10 demonstrates that the Q-PAC packed can be utilized to produce the same quantity of fresh water product but at a lower energy cost. The downside of the Q-PAC is that much more footprint area is needed to achieve the same quantity of production. Despite this

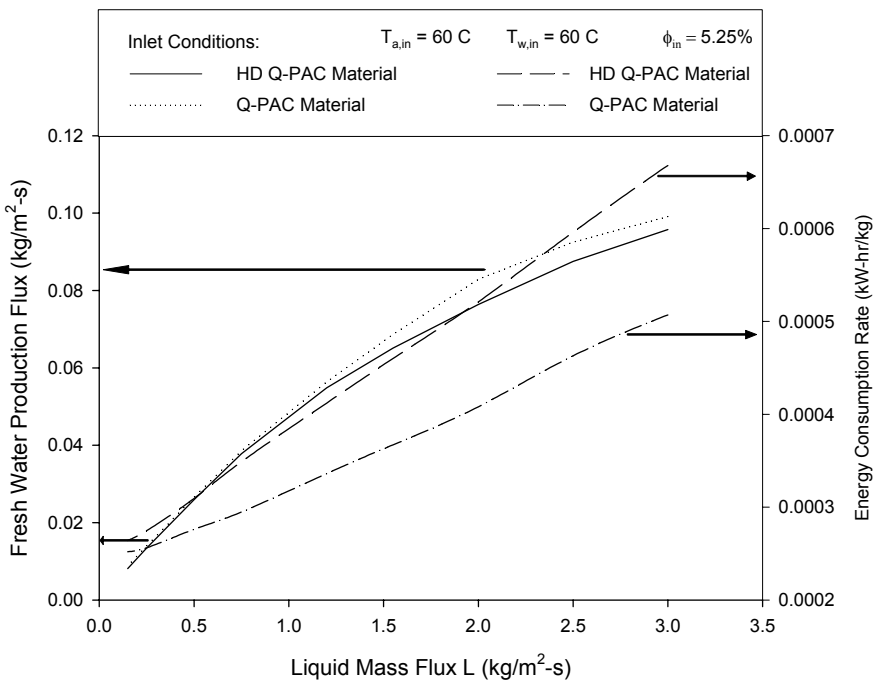

Figure 4-10. Fresh water production flux and energy consumption rate for varying liquid mass flux for HD Q-PAC and Q-PAC packed bed.

fact, however, the Q-PAC could prove to be especially important for large scale DDD facilities. If space is not an issue then the Q-PAC configuration would be advantageous for the lesser energy consumption rate. Further research should be conducted on the Q-PAC to determine the exact wetting and performance.

Industrial Plant Application

In order to fully understand the feasibility of the DDD process with a heated air/heated water input, an economic study must be performed. Consider an industrial plant site that can supply 850,000 acfm of hot air at 82° C (180° F). Figure 4-11 shows a flow diagram of the DDD process coupled with an industrial plant. As the drawing depicts, the waste energy in the form of heated air from the plant site enters the diffusion tower at 82° C. The source brackish/run off/sea water enters the diffusion tower at 30° C. The source water is heated from the water exiting the diffusion tower in a

regenerative heater. The source water will flow down through a packed bed where it will meet the heated air and a portion of the water will evaporate into the air stream. The saturated air exiting the diffusion tower will enter a countercurrent flow oriented direct contact condenser. The fresh water exiting the condenser will enter a fresh water storage tank where a portion is the product and a portion is pumped through a heat exchanger to be cooled and then cycled back to the condenser. For all calculations it is assumed that the sink temperature is 15 °C.

Operation Conditions

Using the analysis described at the beginning of the chapter, Figure 4-12 shows the fresh water production flux for varying diffusion tower liquid mass fluxes. For the analysis the condenser air mass flux is 1.5 kg/m^2-s and the fresh water mass flux is 3.0 kg/m^2-s. These values were determined by Li et al. [11] to be the optimal operating conditions of the direct contact condenser using the HD Q-PAC packing material. It is also assumed that the surface areas of the condenser and diffusion tower are the same. The condenser was analyzed using the model proposed by Li et al. [17]. As seen from Figure 4-12, there is an optimal fresh water production flux for an inlet water temperature of 30 °C at a liquid mass flux of about 0.20 kg/m^2-s. Figure 4-13 depicts the total energy consumption for the DDD process with varying diffusion tower liquid mass flux. From the graph the total energy consumption for an inlet water temperature is optimal in the range of liquid mass fluxes from 0.1-0.2 kg/m2-s. It is fortunate that the optimal total energy consumption and maximum fresh water production occur in the same range. The optimal diffusion tower liquid mass flux is therefore taken to be 0.15 kg/m2-s. It is worthy to note that the energy consumption of the DDD process demonstrated is nearly five times

less than that of reverse osmosis desalination. This is a very distinct advantage to the DDD process.

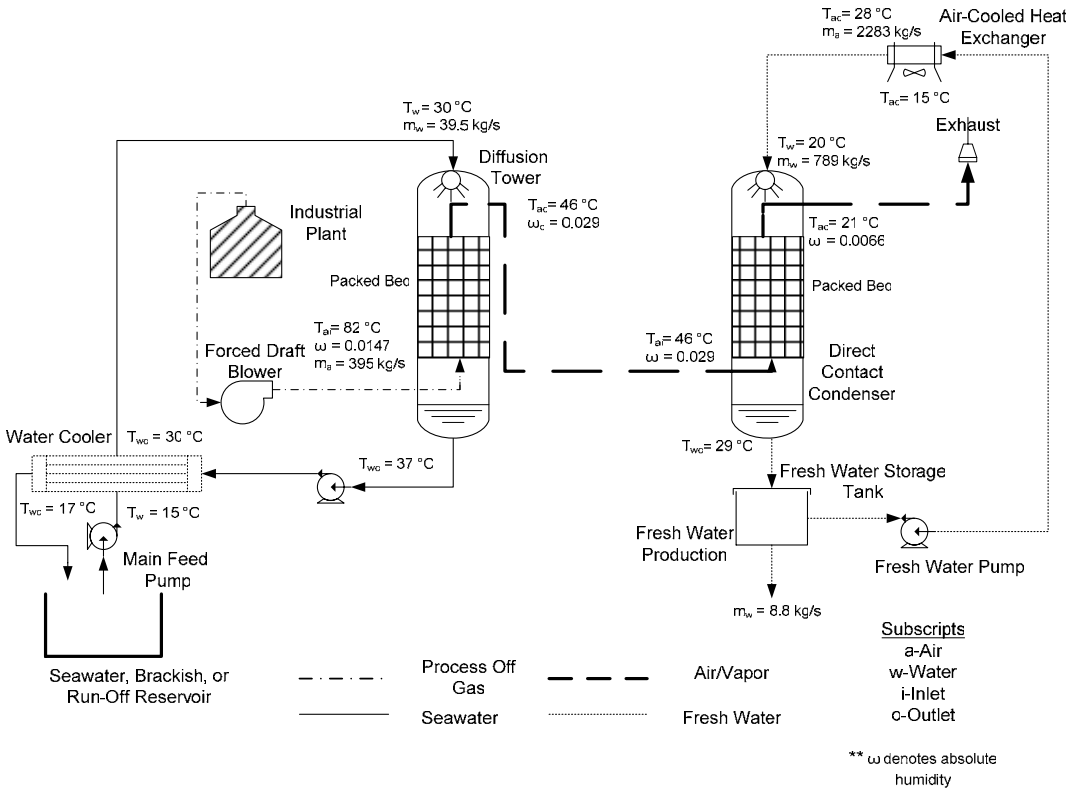

Figure 4-11. Sample schematic of the DDD system coupled with an industrial site.

Figure 4-14 depicts the fresh water production efficiency as a function of diffusion tower liquid mass flux. As the graph shows the fresh water efficiency increases steeply with decreasing diffusion tower liquid mass flux. The fresh water production efficiency in the range of the optimal total energy consumption and fresh water production is quite high and is about 0.224.

The optimal operating conditions of the proposed DDD process coupled with an industrial plant are summarized in Table 4-1. If operating at these conditions there is a potential to produce about 201,800 Gal/day of distilled water with small total electrical

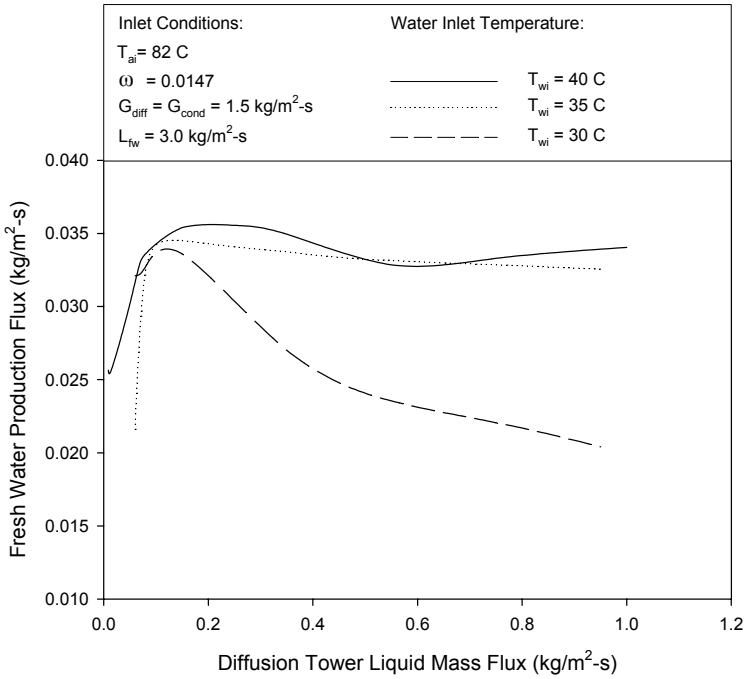

Figure 4-12. Fresh water production flux for varying diffusion tower liquid mass flux.

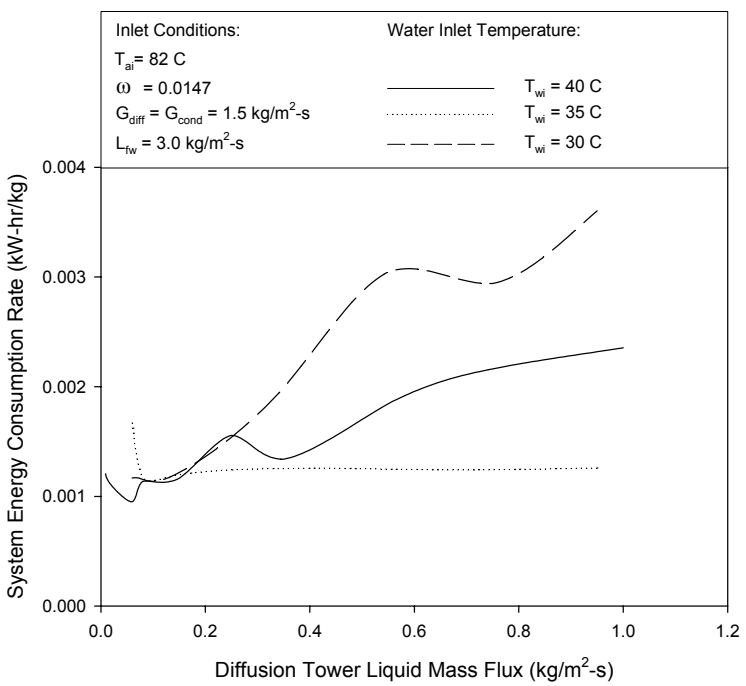

Figure 4-13. Energy consumption rate of the DDD system for varying diffusion tower liquid mass flux.

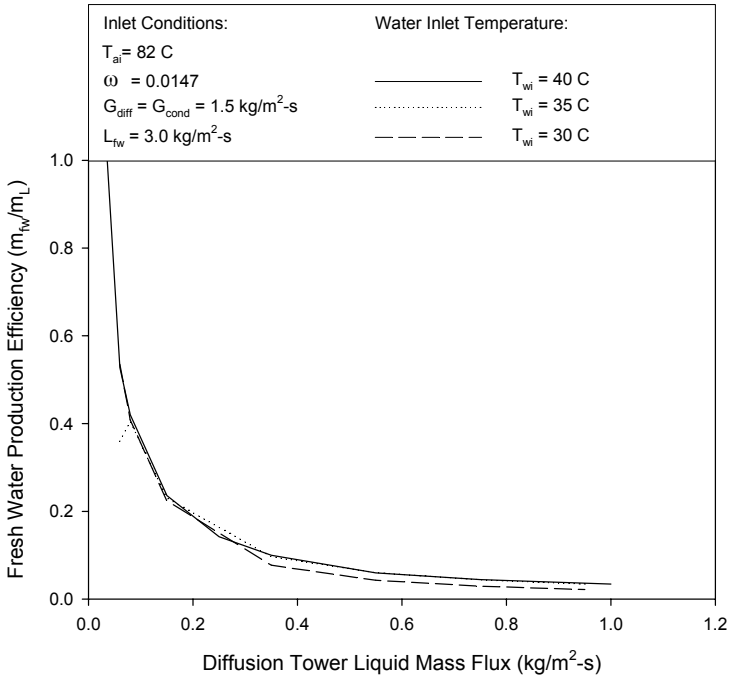

Figure 4-14. Fresh water production efficiency for varying diffusion tower liquid mass flux.

energy consumption of 0.0012 kW-hr/kg and a fresh water production efficiency of 0.224. A total footprint area of 562.3 m^2 is required.

Economic Analysis

Next the cost of the DDD process facility when coupled with an industrial plant is evaluated. The unit cost of a desalination plant is highly dependent upon the site characteristics. Factors such as, plant capacity, pumping units, chemicals, and pretreatment all depend on the given location [21]. According to Ettouney et al. [21] the costs of a desalination facility can be broken down into three segments: direct capital costs, indirect capital costs, and annual operating costs. The direct capital costs include the costs of purchasing the necessary equipment, land, and construction of the plant.

Table 4-1. DDD optimal operating conditions for industrial site.

DDD System Operating Conditions

General Operating Conditions:

Diffusion Tower:	**Condenser:**
$G = 1.5\ kg/m^2\text{-}s$	$G = 1.5\ kg/m^2\text{-}s$
$L = 0.15\ kg/m^2\text{-}s$	$L = 3.0\ kg/m^2\text{-}s$
$T_{ai} = 82°C$	$T_{ai} = 46.05°C$
$T_{wi} = 29.89\ °C$	$T_{wi} = 19.82\ °C$
$\omega_i = 0.01469$	$\omega_i = 0.0290$
$T_{ao} = 46.05\ °C$	$T_{ao} = 21\ °C$
$T_{wo} = 36.95\ °C$	$T_{wo} = 29.2\ °C$
$\omega_o = 0.0290$	$\omega_o = 0.0066$
Height = 0.265 m	Height = 0.822 m

$m_{fw}/_{mL} = 0.224$
$E_{consumption} = 0.001218$ kW-hr/kg
$m_{fw} = 201{,}817$ Gal/day

Flow Conditions using Available Energy (850,000 acfm)

Diffusion Tower:	**Condenser:**
$m_a = 395\ kg/s$	$m_a = 395\ kg/s$
$m_w = 39\ kg/s$	$m_w = 789\ kg/s$
$A_{diff} = 263.16\ m^2$	$A_{cond} = 263.16\ m^2$

1. Land – The cost of land is very region specific. It depends on the demand for land in a given area.

2. Well Construction- Recent studies estimate the cost of construction per meter depth to be $650. The average well capacity is approximated as 500 m^3/d.

3. Process Equipment- This category consists of some of the most expensive equipment all of which will depend upon the plant capacity and process. Instrumentation and controls, pumps, electric wiring, pre-and post-treatment equipment, pipes, valves, and process cleaning systems are all included. The equipment for a RO plant are generally less than that of the distillation processes of MSF. A RO plant equipment can cost as little as $1,000 whereas a MSF plant with a 27,000 m^3/d capacity can cost $40 million.

4. Auxillary Equipment- Generators, transformers, pumps, pipes, valves, wells, storage tanks, and transmission piping are all considered auxillary equipment.

5. Building construction- The building costs are site dependent and can vary from \$100 to \$1,000/m^2.

The indirect costs of a plant are expressed as percentages of the total direct capital cost. The indirect costs include freight and insurance, construction overhead, owner's costs, and contingency costs. The freight and insurance is about 5% of the direct capital costs, construction overhead is about 15% of the direct material and labor costs, owner's costs is 10% of direct material and labor costs, and the contingency costs are about 10% of the total direct costs. The annual operating costs are the costs incurred during plant operation and include electricity, labor, maintenance, insurance, chemicals, and amortization or fixed charges.

The costs for the DDD process operating at the conditions described in Table 4-1 are estimated. The estimates based on the following assumptions:

1. The interesting rate, i, is 5%.

2. The plant life is approximated as n=30 years.

3. The plant availability is estimated as f=0.9.

4. The cost of land is neglected as it assumed that the DDD system will be coupled with an aluminum smelting plant and is readily available.

5. The cost of the chemicals used in pre- or post-treatment of the water is neglected. The cost is neglected because the chemical used in treatment is highly dependent upon the use of the fresh water produced.
6. The specific cost of the operating labor is estimated to be γ = \$0.01/m^3 for the thermal processes and \$0.05/m^3 for RO. Thus for the DDD process the specific cost of the operating labor is approximated as γ = \$0.025/m^3.

7. According to the American Water Works Association [22] the direct costs are estimated to be \$3-\$6/gal per day installed capacity and are determined to be typical seawater desalting plant construction costs. This value does not include any of the off-site construction costs including engineering, legal, or financial

fees. It also does not include the cost to transport the water to the plant, or incidental or contingency costs. However the cost to develop the site is included and is estimated to be 5% of the material and construction costs.

The amortization factor is calculated as,

$$a = \frac{i(1+i)^n}{(1+i)^n - 1} \ , \tag{4.8}$$

where i is the interest rate and n is the plant life. The annual fixed costs are calculated as,

$$A_{fixed} = (a)(DC) \ , \tag{4.9}$$

where DC is the direct capital cost. Lastly, the annual labor cost is evaluated as,

$$A_{labor} = (\gamma)(f)(m)(365) \ , \tag{4.10}$$

where γ is the specific cost of operating labor and m is the plant capacity (m^3/day). Therefore the total annual cost can be calculated as,

$$A_{total} = A_{fixed} + A_{labor} \tag{4.11}$$

It should be noted that the cost of the waste heat, for this case in the form of heated air, is not included since it is waste that would have otherwise been discarded into the environment. Therefore the unit product cost of the system is calculated as follows,

$$A_{unit,p} = \frac{A_{total}}{f \cdot m \cdot 365} \tag{4.12}$$

Table 4-2 summarizes the estimate of the direct costs for a full scale diffusion driven desalination facility operating in conjunction with an industrial plant. The analysis shows that the production cost, neglecting the electricity charges, is between 0.19-0.36 \$/m^3. In terms of \$/10^3 gal the production cost is 0.72-1.34 \$/10^3 gal.

The fresh water profit is the most important consideration in the analysis of the DDD facility. One of the most expensive operating costs is the pumping power required

Table 4-2. Summary of DDD Plant Costs.

Unit	Calculated Result
Direct Costs (10^3 \$)	636-1,271
AC_{fixed} (10^3 \$)	41-83
A_{labor} (10^3 \$)	6.3
$A_{labor}+AC_{fixed}$ (10^3 \$)	47.7-89
$AC_{unit,p}$(\$/m^3)	0.19-0.36

to operate the pumps and the blowers. It is not included in the summary of costs listed in Table 4-2. Since the cost of electricity is highly fluctuating it is factored into the determination of the profit. The fresh water profit can be calculated as,

$$\prod_f = Q_f - AC_{unit,p} - Pw_f Q_{elec}\,, \tag{4.13}$$

where $\prod_f$ (\$/10^3gal) is the net fresh water profit, $AC_{unit,p}$ (\$/10^3gal) is the production cost calculated above, Q_f (\$/10^3gal) is the retail price of fresh water, and Q_{elec} (\$/kW-hr) is the retail price of electricity. Here $AC_{unit,p}$ is taken to be an intermediate value of \$0.99/10^3gal. The profit to be gained is highly dependent on the retail cost of water and the cost of water strongly depends on how the water is transported to the customer. Two different scenarios will be evaluated. First, the profit will be evaluated when the water is transferred to the customer via municipal pipelines. For this case, Figure 4-15 depicts the calculated net fresh water profit as a function of the retail price of electricity for varying costs of water. On average, the retail price of water in the United States is about \$3/10^3gal. For this price, the largest profit to be earned is for the lowest energy retail price of \$0.04/kW-hr. As the retail price of energy increases, the profit linearly decreases. A similar trend is observed for the other water retail prices. If the retail price

of water is $\$3/10^3$gal and the cost of electricity is \$0.08/kW-hr, then the profit is about $\$1.80/10^3$gal. For the production summarized in Table 4-1, this amounts to a profit of only \$363/day. Given this profit outlook it advantageous to consider other prospects to market the product distilled water.

It is of importance to recall that the product of the DDD process is high purity distilled water, which is of superior quality to that circulating through the municipal lines. Another possible solution therefore would be to consider selling the distilled water as bottled water. Figure 4-16 shows the growth of the bottled water industry. As the graph shows, the sale of bottled water has been steadily increasing since the late 1970s. Clarke and King [1] estimate that the bottled water market was worth an estimated \$20 billion a year for 2002 alone. The reasons for the increase in bottled water consumption vary from distaste of tap water, distrust of the safety of tap water, and the overall realization that water is a healthier choice of beverage than soda and other carbonated beverages. The price per gallon of bottled distilled water can vary between \$0.90-\$1.50 per gallon. Without taking into account the cost of bottling, Figure 4-17 shows the net fresh water profit that can be achieved with the DDD fresh water product. The graph shows that the operating and production costs have little effect on the fresh water profit. Nearly all revenue generated from sales is considered profit. If the distilled bottled water is sold at \$1.00/gal and the DDD process can produce 201,800 gal/day then the profit generated is about \$200,000/day or \$73 million/yr. As it can be seen there is the possibility of enormous profit because the profit is basically the retail price of the distilled bottled water. Given the continuous growth of the bottled water industry that shows no signs of slowing down, an enormous profit can be rendered from the DDD process.

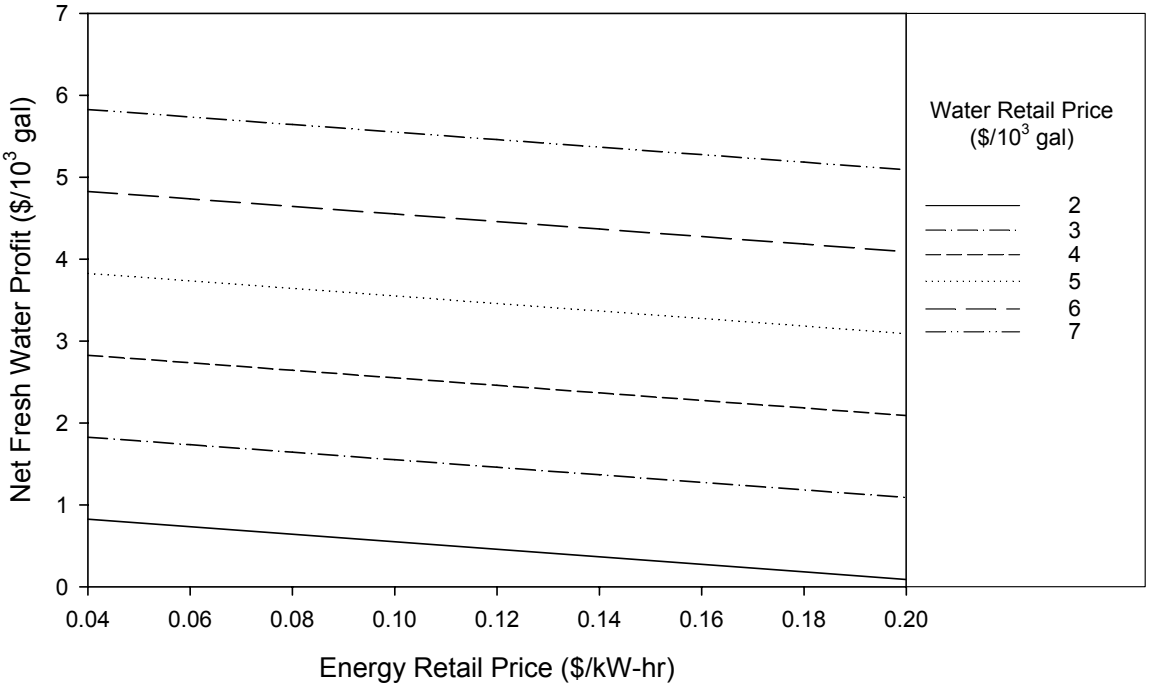

Figure 4-15. Net fresh water profit as a function of energy retail price for varying water retail price.

Overall the DDD process utilizing a heated air/heated water inlet conditions has proven to be an economically reasonable process when coupled with an industrial plant that can provide waste heat. While transporting the distilled fresh water product to customers predicted minimal profit, the bottled water industry provides the opportunity to sell the distilled water for enormous profit.

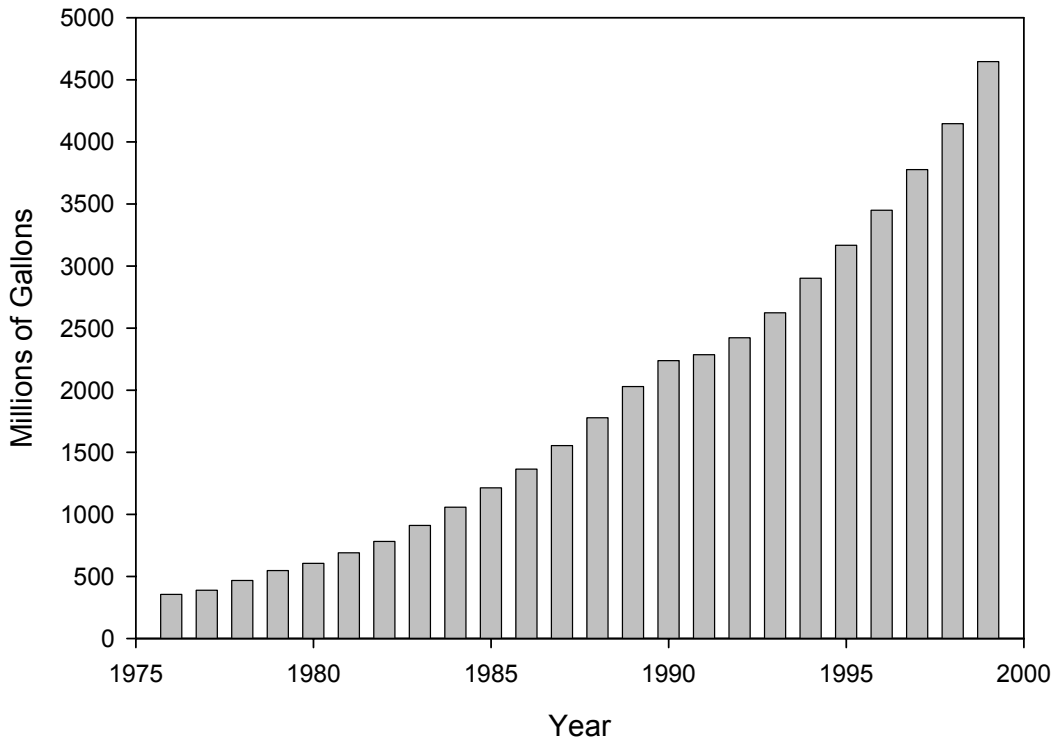

Figure 4-16. The bottled water market in the United States [23].

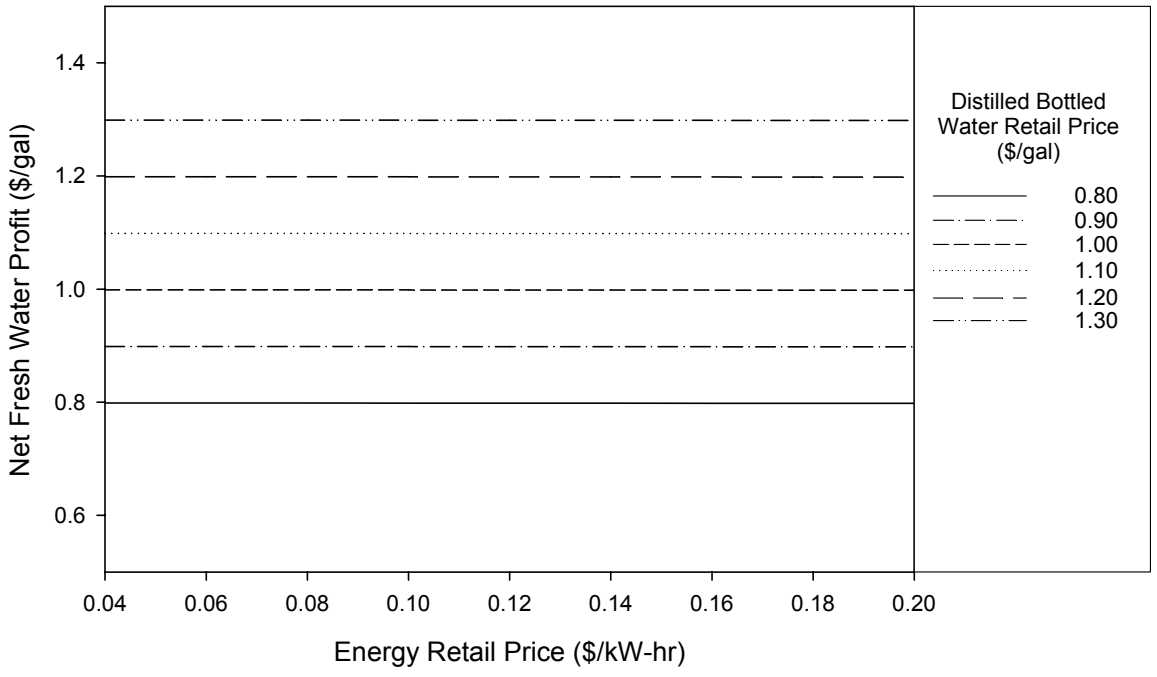

Figure 4-17. Net fresh water product as a function of energy retail price for varying distilled bottled water prices.

CHAPTER 5
CONCLUSION

The diffusion driven desalination process provides an economic means for utilizing and converting saltwater to high purity distilled water A laboratory scale DDD facility has been designed and constructed which is fully instrumented and includes a data acquisition system. The laboratory facility has been modified to include an air heating section which heats the inlet air flowing to the diffusion tower. Experiments were conducted on the diffusion tower for two different cases: the heated air/ambient water and heated air/heated water. For each case, a set of experiments were conducted by holding the air mass flux constant and varying the liquid mass flux over a range of values.

The heat and mass transfer for the DDD process were analyzed. A one dimensional liquid film model was used to obtain three coupled ordinary differential equations with dependent variables of humidity, water temperature and air temperature. Closure was achieved by using the heat and mass transfer analogy and Onda's correlation was used to evaluate the mass transfer coefficients. Through experimental analysis, the wetted specific area of the packed bed was found to be a constant in the range of operating conditions studied. It was also found that for the heated air/heated water case there is moderate heat loss from the system that must be accounted for in the energy balance. The experimental values obtained were compared to those obtained from the theoretical heat and mass transfer model. Agreement between the two was quite good for both cases. It was also found that the repeatability of the experiments is satisfactory. The

heated air/ambient water case proved to be inefficient with very little change in exit conditions over the range of liquid and air mass fluxes. The heated air/heated water process proved to give better performance. The theoretical model is a necessary tool needed to design an efficient DDD facility.

A parametric study to determine the effect of certain operating variables on the maximum freshwater production was completed for the heated air/heated water DDD process. For each liquid mass flux there is an optimal air mass flux where the maximum fresh water production flux is produced. There is also a location where the energy consumption for pumping through the diffusion tower is minimized.

The heated air/heated water process was compared to other different DDD processes, specifically the heated water/ambient air case and the heated air/heated water process utilizing the Q-PAC packed bed, a less dense and lower pressure drop packing material. The comparison showed that the heated air/heated water DDD process has its advantages and disadvantages at different operating conditions. In comparison for the heated water/ambient air it was shown that the heated air/heated water process requires more electrical energy than the heated water/ambient air process at low liquid mass flux however the fresh water production efficiency for the heated air/heated water is greater for all values of liquid mass flux. The fresh water production for the heated air/heated water process is greater for all liquid mass flux. In the comparison with the heated air/heated water using the Q-PAC packing, it was shown that similar fresh water production can be achieved at a lower energy cost by using Q-PAC. Further studies are required to determine the wettability of Q-PAC and its wetted fraction as part of the DDD process.

An economic study was performed to determine the cost effectiveness of the DDD process using a heated air/heated water input when coupled with an industrial plant producing waste heat in an air stream. If 850,000 acfm of 82 °C heated waste heat in air is available from a plant the optimal operating conditions are a diffusion tower liquid mass flux of 0.15 kg/m^2-s, an air mass flux of 1.5 kg/m^2-s, and a fresh water mass flux of 3.0 kg/m^2-s in the condenser. At these conditions with the given amount of waste heat available, the plant can produce 201,800 gal/day of high purity distilled water while consuming a miniscule 0.0012 kW-hr/kg and having a fresh water conversion efficiency of 0.224. Through an economic study it was determined that a reasonable profit can be realized by selling the product as distilled bottled water. Without taking into account the cost of bottling, assuming that a gallon of distilled water costs $1.00 per gallon, a profit of $0.99 per gallon can be achieved.

Extensive research has already been performed on the DDD process and while the future of the process looks optimistic, further research needs to be done. The DDD process needs to be further examined on a larger scale. A pilot facility should be constructed and the DDD performance should be analyzed over long term operation in an industrial setting. As of yet, the DDD process has not been analyzed using a saline feed water source in the diffusion tower. Using such a source, water quality testing of the fresh water produced in the DDD process should be conducted. This is important in determining what type of post treatment of the product water is required.

The DDD process has been thoroughly studied using a laboratory scale facility. The diffusion tower performance has been studied for heated air/heated water, heated air/ambient water, and heated water/ambient air inputs [16]. On a small scale, further

experiments should be conducted to determine the performance of DDD system utilizing a different type of packed bed. On a larger scale, the DDD process now needs to be examined with a pilot scale facility coupled with a low grade waste heat source to determine its performance under an industrial load and continuous operation.

APPENDIX A
ONDA'S CORRELATION

$$k_L = 0.0051 \mathrm{Re}_{Lw}^{2/3} Sc_L^{-0.5} \left(ad_p\right)^{0.4} \left[\frac{\mu_L g}{\rho_L}\right]^{1/3}$$

$$k_G = C \mathrm{Re}_{GA}^{0.7} Sc_G^{1/3} \left(ad_p\right)^{-2} aD_G$$ **,** (C=5.23 if d_p > 15 mm; C=2 if $d_p \leq$ 15 mm)

$$^{*}\ a_w = a\left\{1 - \exp\left[-2.2\left(\frac{\sigma_c}{\sigma_L}\right)^{3/4} \mathrm{Re}_{LA}^{1/2} Fr_L^{-0.05} We_L^{1/5}\right]\right\}$$

$$\mathrm{Re}_{LA} = \frac{L}{a\mu_L},\ Fr_L = \frac{L^2 a}{\rho_L g},\ We_L = \frac{L^2}{\rho_L \sigma_L a}$$

$$\mathrm{Re}_{LW} = \frac{L}{a_w \mu_L}, \mathrm{Re}_{GA} = \frac{G}{a\mu_G},\ Sc_L = \frac{\mu_L}{\rho_L D_L},\ Sc_G = \frac{\mu_G}{\rho_G D_G}$$

* This equation has been modified from Onda's original correlation

APPENDIX B
EXPERIMENTAL DATA OF THE DIFFUSION TOWER FOR HEATED AIR/AMBIENT WATER

m_L (kg/s)	m_a (kg/s)	$T_{L,in}$ (° C)	$Ta_{,in}$ (° C)	ω_{in}	$T_{L,out}$ (° C)	$T_{a,out}$ (° C)	ω_{out}
0.031	0.040	25.26	59.83	0.0075	26.93	26.07	0.0206
0.040	0.040	25.36	60.26	0.0075	26.98	25.95	0.0205
0.047	0.040	25.30	59.88	0.0075	26.87	25.80	0.0203
0.056	0.040	25.36	60.27	0.0075	26.94	25.75	0.0203
0.063	0.040	25.30	60.27	0.0075	26.80	25.70	0.0203

m_L (kg/s)	m_a (kg/s)	$T_{L,in}$ (° C)	$Ta_{,in}$ (° C)	ω_{in}	$T_{L,out}$ (° C)	$T_{a,out}$ (° C)	ω_{out}
0.028	0.040	25.28	61.82	0.0041	25.70	26.04	0.0201
0.035	0.040	25.30	61.91	0.0040	25.70	25.58	0.0198
0.044	0.041	25.09	61.66	0.0041	25.42	25.11	0.0194
0.059	0.041	25.10	61.76	0.0041	25.38	24.99	0.0193

m_L (kg/s)	m_a (kg/s)	$T_{L,in}$ (° C)	$Ta_{,in}$ (° C)	ω_{in}	$T_{L,out}$ (° C)	$T_{a,out}$ (° C)	ω_{out}
0.029	0.060	25.30	60.57	0.0060	26.73	26.04	0.0204
0.039	0.060	24.77	60.82	0.0061	26.45	25.66	0.0200
0.051	0.060	25.06	60.95	0.0062	26.40	25.65	0.0200
0.062	0.059	25.33	61.33	0.0062	26.40	25.70	0.0201

m_L (kg/s)	m_a (kg/s)	$T_{L,in}$ (° C)	$Ta_{,in}$ (° C)	ω_{in}	$T_{L,out}$ (° C)	$T_{a,out}$ (° C)	ω_{out}
0.032	0.060	24.90	60.38	0.0068	26.29	26.09	0.0205
0.039	0.061	25.25	59.78	0.0067	26.38	25.86	0.0203
0.043	0.061	25.20	59.83	0.0068	26.43	25.86	0.0203
0.049	0.060	25.20	59.95	0.0069	26.48	25.83	0.0203
0.055	0.060	25.17	60.03	0.0069	26.35	25.81	0.0203
0.064	0.061	25.16	60.16	0.0069	26.28	25.79	0.0203

m_L (kg/s)	m_a (kg/s)	$T_{L,in}$ (° C)	$Ta_{,in}$ (° C)	ω_{in}	$T_{L,out}$ (° C)	$T_{a,out}$ (° C)	ω_{out}
0.029	0.080	24.66	61.09	0.0068	27.49	26.34	0.0207
0.037	0.081	25.09	61.03	0.0072	27.46	26.32	0.0208
0.048	0.081	25.39	60.96	0.0071	27.37	26.25	0.0208
0.055	0.080	25.17	61.09	0.0072	27.27	26.16	0.0207
0.065	0.081	25.38	61.39	0.0073	27.33	26.21	0.0208

m_L (kg/s)	m_a (kg/s)	$T_{L,in}$ (° C)	$Ta_{,in}$ (° C)	ω_{in}	$T_{L,out}$ (° C)	$T_{a,out}$ (° C)	ω_{out}
0.035	0.080	25.28	60.38	0.0080	27.51	26.67	0.0213
0.042	0.080	25.27	60.30	0.0081	27.40	26.68	0.0213
0.048	0.080	25.34	60.43	0.0080	27.37	26.61	0.0213
0.056	0.079	25.24	60.76	0.0080	27.31	26.55	0.0212
0.065	0.081	25.27	60.46	0.0080	27.13	26.42	0.0211

APPENDIX C
EXPERIMENTAL DATA OF THE DIFFUSION TOWER FOR HEATED AIR/HEATED WATER

m_L (kg/s)	m_a (kg/s)	$T_{L,in}$ (° C)	$Ta_{,in}$ (° C)	ω_{in}	$T_{L,out}$ (° C)	$T_{a,out}$ (° C)	ω_{out}
0.034	0.040	60.82	61.03	0.0066	37.21	42.28	0.0550
0.039	0.039	60.99	61.15	0.0066	37.81	43.57	0.0591
0.047	0.039	59.99	61.71	0.0066	38.84	44.74	0.0632
0.054	0.040	60.58	60.94	0.0069	39.96	44.76	0.0631
0.061	0.041	61.02	60.61	0.0071	40.41	45.54	0.0661
0.068	0.041	59.48	60.52	0.0074	40.91	45.03	0.0642

m_L (kg/s)	m_a (kg/s)	$T_{L,in}$ (° C)	$Ta_{,in}$ (° C)	ω_{in}	$T_{L,out}$ (° C)	$T_{a,out}$ (° C)	ω_{out}
0.036	0.041	61.00	61.35	0.0059	35.99	42.30	0.0566
0.043	0.040	60.79	61.57	0.0059	36.27	44.03	0.0624
0.050	0.040	60.75	61.69	0.0061	37.30	44.71	0.0649
0.056	0.041	60.89	61.53	0.0064	39.12	44.10	0.0627
0.064	0.042	60.31	60.94	0.0066	39.63	44.89	0.0656

m_L (kg/s)	m_a (kg/s)	$T_{L,in}$ (° C)	$Ta_{,in}$ (° C)	ω_{in}	$T_{L,out}$ (° C)	$T_{a,out}$ (° C)	ω_{out}
0.032	0.059	61.01	61.10	0.0078	33.65	37.74	0.0420
0.041	0.060	61.66	61.08	0.0078	34.46	39.70	0.0474
0.047	0.061	61.12	60.93	0.0080	35.02	40.20	0.0489
0.055	0.060	60.05	61.23	0.0079	36.14	40.98	0.0511
0.063	0.059	60.52	62.10	0.0081	39.87	42.18	0.0550

m_L (kg/s)	m_a (kg/s)	$T_{L,in}$ (° C)	$Ta_{,in}$ (° C)	ω_{in}	$T_{L,out}$ (° C)	$T_{a,out}$ (° C)	ω_{out}
0.033	0.061	60.79	60.52	0.0080	32.46	37.51	0.0416
0.038	0.060	60.76	60.69	0.0080	33.51	38.44	0.0448
0.046	0.060	60.97	61.03	0.0081	34.65	39.70	0.0482
0.056	0.061	60.86	61.10	0.0082	35.95	40.85	0.0498
0.062	0.060	60.57	61.16	0.0083	37.06	41.33	0.0510

m_L (kg/s)	m_a (kg/s)	$T_{L,in}$ (° C)	$Ta_{,in}$ (° C)	ω_{in}	$T_{L,out}$ (° C)	$T_{a,out}$ (° C)	ω_{out}
0.030	0.080	60.94	60.11	0.0088	30.75	34.51	0.0353
0.039	0.080	61.01	60.29	0.0090	31.88	35.91	0.0387
0.048	0.080	60.45	60.48	0.0088	33.04	37.40	0.0426
0.056	0.081	60.40	60.78	0.0089	34.88	38.02	0.0442
0.066	0.080	60.26	60.94	0.0090	36.02	39.01	0.0468

m_L (kg/s)	m_a (kg/s)	$T_{L,in}$ (° C)	$Ta_{,in}$ (° C)	ω_{in}	$T_{L,out}$ (° C)	$T_{a,out}$ (° C)	ω_{out}
0.032	0.080	59.69	59.94	0.0080	31.03	35.02	0.0350
0.036	0.080	61.29	59.73	0.0083	30.82	35.97	0.0378
0.046	0.080	60.83	61.09	0.0084	32.97	37.12	0.0410
0.055	0.081	60.57	60.96	0.0086	34.43	37.90	0.0429
0.064	0.081	58.98	60.40	0.0088	34.99	38.97	0.0458

LIST OF REFERENCES

1. Clarke, R., and King, J., 2004, *The Water Atlas*, The New Press, New York.

2. Semiat, R., 2000, "Desalination: Present and Future," Water International, **25**(1), pp. 54-65.

3. Dore, M., 2005, "Forecasting the Economic Costs of Desalination Technology," Desalination., **172**, pp. 207-214.

4. Ehrenman, G., April 2003, "Mapping the Road to Water," Mechanical Engineering, **125**(4), pp. 23.

5. Economic and Social Commission for Western Asis, 2001, "Energy Options for Water Desalination in Selected ESCWA Countries," Publication E/ESCWA/ENR/2001/17, United Nations, New York.

6. Bourouni, K., Chaibi, M.T., Tadrist, L., 2001, "Water Desalination by Humidification and Dehumidification of Air: State of the Art," Desalination, **137**, pp. 167-176.

7. Bourouni, K., Martin, R., Tadrist, L., Chaibi, M.T., 1999, "Heat Transfer and Evaporation in Geothermal Units," Applied Science, **64**, pp. 129-147.

8. Al-Hallaj, S., Farid, M.M., Tamimi, A.R., 1998, "Solar Desalination with a Humidification-Dehumidification Cycle: Performance of the Unit," Desalination, **120**, pp. 273-280.

9. Vlachogiannis, M., Bontozoglou, V., Georgalas, C., Litinas, G., 1999, "Desalination by Mechanical Compression of Humid Air," Desalination, **122**, pp. 35-42.

10. Klausner, J.F., Li Y., Darwish, M., and Mei, R., 2004, "Innovative Diffusion Driven Desalination Process", J. of Energy Resources Technology, **126**(3), pp. 219-225.

11. Li, Y., Klausner, J.F., Mei, R., 2006, "Performance Characteristics of the Diffusion Driven Desalination Process", Desalination, **196**, pp. 188-209.

12. Sadhawani, J.J., Veza, J.M., Santana, C., 2005, "Case Studies on Environmental Impact of Seawater Desalination," Desalination, **185**, pp. 1-8.

13. Morton, A.J., Callister, I.K., Wade, N.M., 1996, "Environmental Impacts of Seawater Distillation and Reverse Osmosis Processes," Desalination, **108**, pp. 1-10.

14. Breschi, D., 1999, "Seawater Distillation from Low-Temperature Streams: A Case History," Desalination, **122**, pp. 247-254.

15. Li, Y., 2006, "Heat and Mass Transfer for the Diffusion Driven Desalination Process," Ph.D. Thesis, University of Florida, Gainesville.

16. Klausner, J. F., Li, Y., Mei, R., 2006, "Evaporative Heat and Mass Transfer for the Diffusion Driven Desalination Process," J. of Heat and Mass Transfer, **42**, pp. 528-536.

17. Li, Y., Klausner, J., Mei, R., Knight, J., 2006, "Direct Condensation in Packed Beds," International J. of Heat and Mass Transfer, **49**, pp. 4751-4761.

18. Kays, W.M., Crawford, M.E., Weigand, B., 2005, *Convective Heat and Mass Transfer*, McGraw Hill, New York.

19. Eckert, E.R.G., Goldstein, R.J., 1976, *Measurements in Heat Transfer*, Hemisphere Publishing Corp, Washington, Chap. 9.

20. Onda, K., Takechi, H., Okumoto, Y., 1968, "Mass Transfer Coefficients Between Gas and Liquid Phases In Packed Columns", J. Chem. Eng. Jpn., **1**, pp. 56-62.

21. Ettouney, H. M., El-Dessouky, H. T., Raibish, R. S., Gowin, P. J., December 2002, "Evaluating the Economics of Desalination," Chemical Eng. Prog., **98**(12), pp. 32-39.

22. Water Desalting Committee of the American Water Works Association., 2004, *Water Desalting Planning Guide For Water Utilities*, John Wiley & Sons, Inc, New Jersey.

23. International Bottled Water Association, 2000, "U.S. Bottled Water Market Volume, Growth, Consumption -- 1976-1999," 2000 Marketing Report Findings, Retrieved on November 17, 2006 from http://www.bottledwater.org/public/statistics_main.htm.

BIOGRAPHICAL SKETCH

Jessica Knight is the daughter of Donald and Renee Knight. She was born and raised in Jacksonville, Florida. She began attending the University of Florida in August 2000 where she later earned her bachelor's degree in mechanical engineering in December 2004. She began working on the diffusion driven desalination project in her senior year of her undergraduate studies. She continued research on the diffusion driven desalination process as a graduate student in January 2005 in pursuit of a Master of Science degree.